THE DEVELOPMENT OF A NORMALIZED RADAR CROSS SECTION MODEL FOR ICEBERGS

BYRON REGINALD DAWE

THE DEVELOPMENT OF A NORMALIZED RADAR CROSS SECTION MODEL FOR ICEBERGS

by

Byron Reginald Dawe, B. Eng.

A Thesis submitted in partial fulfillment of
the requirements for the degree of
Master of Engineering

Faculty of Engineering
Memorial University of Newfoundland

December, 1983

St. John's Newfoundland

ISBN 0-315-33614-5

ABSTRACT

To reliably assess the detection performance of marine radars against iceberg targets a realistic model of the normalized radar cross section is required. Previous research indicates that the radar cross section of an iceberg is directly proportional to the area of an iceberg projected onto a plane normal to the radar beam and that aspect and overall shape are secondary factors. Physical descriptions of the iceberg surface indicate that in the X-band and K_u-band frequency range an iceberg can be modelled as a target composed of a number of large (on the wavelength scale) slightly rough (on the wavelength scale) surfaces. Empirical fitting of K_u-band scatterometer data (measured normalized radar cross section values) to an average incoherent normalized radar cross section statistical model for a slightly rough surface employing a Gaussian surface height correlation coefficient shows that such a model is applicable to a slightly rough iceberg surface. The model at 9.5 GHZ (horizontal polarization) is shown to give good agreement with independent measurements made by other researchers after making some general assumptions. It predicts that vertical polarization will give higher normalized cross sectional values. Higher frequencies will give higher values for incidence angles less than about 50° from the vertical. Through the use of standard target modelling techniques this normalized radar

cross sectional model can be applied in a practical manner to provide a quantitative assessment of the detection capability of icebergs on current commercially available marine radars.

ACKNOWLEDGEMENTS

Appreciation is expressed for the fellowship provided by the Centre for Cold Ocean Resources Engineering, which allowed me to initiate my graduate studies. I also express my thanks to the Faculty of Engineering for it's support and patience in allowing me to see my graduate studies through to a successful completion. In particular, I thank Dr. Denes Bajzak and Dr. John Walsh, my joint supervisors. I also thank Wanda Tucker for doing an excellent job of typing this thesis. Last, but by no means least, I thank my wife, Margaret, for her perseverance, unwavering support and limitless patience which ultimately allowed me to complete this work.

TABLE OF CONTENTS

LIST OF TABLES

LIST OF FIGURES

CHAPTER 1

THE PROBLEM

1.1 THE ICEBERG PHENOMENA

Icebergs are formed by the calving of glaciers. The primary sources of icebergs (85 percent) off the east coast of Canada are the West Greenland glaciers. The remaining sources are the East Greenland glaciers (10 percent) and the ice shelves of the northern part of Ellesmere Island (Dinsmore, 1972). The predominant ocean currents between the west coast of Greenland and the east coasts of the Ellesmere, Devon and Baffin Islands cause icebergs produced on the West coast of Greenland to drift north along the Greenland coast, west across Melville Bay and then south along the east coasts of the Ellesmere, Devon and Baffin Islands. The Ellesmere Island icebergs join this procession at the most northern point. The East Greenland icebergs round the southern tip of Greenland with some drifting directly westward across the Davis Strait and then south, while the remainder drift north deteriorating rapidly in the warm West Greenland current.

Dinsmore (1972) reports that approximately 15,000 icebergs are calved each year from the West Greenland glaciers. An average of about 1000 icebergs reach as far south as the Strait of Belle Isle while about 400 reach the

northern part of the Grand Banks. The actual number reaching these areas can vary quite considerably. Continuous melting results in eventual total disintegration, with the maximum southern extent usually being the southern Grand Banks region. The "iceberg season" off Newfoundland usually extends from April to July, while off Labrador and further north icebergs may be present on a year round basis.

Icebergs range in size from small insignificant pieces to sizes in the order of many millions of tonnes, and their above water portions take on a multitude of shapes, with no one iceberg having exactly the same shape as another. Their specific gravity (averaging between 0.85 and 0.90 grams per cubic centimetre) results in almost ninety percent of their mass being under water. The continuous melting and the force of the winds, waves and currents cause them to become unstable and roll unpredictably. They can also calve unpredictably into two or more smaller icebergs.

1.2 THE THREAT

Glacial ice is a very hard material, therefore icebergs pose a significant environmental hazard to the marine transportation, fishing, and offshore hydrocarbon industries. A collision between a vessel or an offshore platform and an iceberg can result in severe damage being sustained or even a sinking. As a result of the increased

hydrocarbon exploration in the Eastern Canadian Arctic, off the coast of Labrador and off Newfoundland, marine traffic and offshore drilling activity has increased considerably. The probability of the installation of large offshore production platforms and the utilization of both giant liquid natural gas carriers and oil tankers highlights the need for methods to reliably monitor iceberg locations and micro and macro drift trajectories. Indeed, Duval (1975) stated that icebergs posed the most serious environmental threat to offshore drilling activity in the Labrador Sea, while Blenkarn and Knapp (1975) considered them to be the most dramatic phenomena facing drilling activity on the Grand Banks.

1.3 CURRENT ICEBERG MONITORING TECHNIQUES

In 1912 the "unsinkable" passenger liner, the "S.S. Titanic", sank after colliding with an iceberg about 200 nautical miles northeast of Newfoundland. A considerable loss of life resulted. This catastrophy precipitated in the formation of the International Ice Patrol (IIP), an organization operated by the United States Coast Guard (USCG) and funded by a number of countries. The primary responsibility of the IIP is to monitor and report to mariners the locations of the icebergs that frequent the shipping lanes and fishing areas off the east coast of Newfoundland. They rely on aircraft and ship observations for their information. The poor weather conditions which

frequent the area during the iceberg season makes this task extremely difficult. The USCG has derived an iceberg classification system which is used by the IIP and adopted by the World Meteorological Organization. The system is based on the size and shape of the above water portion of the iceberg. Table 1 shows the classification system.

The need for reliable shipboard tracking of icebergs under all weather day or night conditions is evident. In 1935 the French liner "Normandie" was the first commercial vessel to be equipped with a civil marine radar (Williams, 1979). Because of radar's almost all weather day or night detection capability, it was initially thought to be of considerable value in detecting and tracking icebergs. However, a number of studies and numerous observations have shown it to be less reliable than initially believed. The current requirement of highly reliable close tactical monitoring of icebergs necessitates an accurate quantitative evaluation of the utility of marine radar.

1.4 RESEARCH OBJECTIVE

This research was specifically concerned with the development of a realistic X-band normalized radar cross section model for an iceberg surface. Specifically, the frequency of interest was 9.5 Gigahertz (GHz) which is commonly used in commercial marine radars. There have been a number of studies undertaken over the past forty years

TABLE 1 - ICEBERG SIZE/SHAPE CLASSIFICATION SYSTEM (Murray, 1969)

1. (a) Size (all types but tabular):

S — SMALL — height less than 50 ft; length less than 200 ft.
M — MEDIUM — height 50-150 ft; length 200-400 ft.
L — LARGE — height 150-255 ft; length 400-700 ft.
VL — VERY LARGE — height greater than 255 ft; length greater than 700 ft.

(b) Tabular bergs:

S — SMALL — height 20 ft; length less than 300 ft.
M — MEDIUM — height 20-50 ft; length 300-700 ft.
L — LARGE — height greater than 50 ft; length greater than 700 ft.

Note: Sizes refer to the above-water portion only. If the height and length of a berg falls into a different size classification, the larger size is used.

2. Type

(a) BLOCKY (B) — Steep precipitous sides with horizontal or flat top. Very solid berg. Length-height ratio 5:1.
(b) DRYDOCK (DK) — Eroded such that a large U-shaped slot is formed, with twin columns or pinnacles. Slot extends into the water line or close to it.
(c) DOME (D) — Large smooth rounded top. Solid-type berg.
(d) PINNACLED (P) — Large central spire or pyramid of one or more spires dominating shape. Less massive than dome-shaped berg of similar dimensions.
(e) TABULAR (T) — Horizontal or flat-topped berg with length-height ratio of 5:1.
(f) BERGY BIT — A mass of glacial ice smaller than a berg but larger than a growler, about the size of a small cottage. Small berg or large growler is preferred usage
(g) GROWLER — A mass of glacial ice that has calved from a berg or is the remains of a berg. A growler has a height of less than 8 ft and a length of less than 20 ft.

which examined both quantitatively and qualitatively the detection of icebergs by marine radar. Although the factors affecting the detection of a marine target from a shipborne marine radar are well known a key limitation in assessing their perfotmance is the lack of knowledge regarding the radar cross section of an iceberg. None of these studies have involved the development of a general normalized radar cross section model which has been verified by measured results and can be used to determine the total radar cross section of an iceberg.

The research objective here was to develop just such a model. It involved a review of the principles of operation of a marine radar and the factors affecting its performance, a comprehensive review of the literature describing the radar detection of icebergs, with the extraction of relevant data, and the development of a X-band normalized radar cross section model for an iceberg. Methods by which the model can be applied were also examined.

CHAPTER 2

MARINE RADAR

2.1 INTRODUCTION

This chapter concerns itself with the basic principles of operation of a commercial marine radar. A detailed discussion of the radar equation is also included. The effect of various environmental factors are also described.

2.2 BASIC DESCRIPTION

Marine radar is an active microwave remote sensing device. Standard commercial radars transmit energy in the pulsed continuous wave radar mode. In this mode a short burst of electromagnetic energy is transmitted (typically 1 microsecond long or less) periodically. The pulse consists of a number of cycles of electromagnetic energy at one frequency. The time delay between transmission of the pulse and the return of the reflected pulse from a target is used to determine the range to the target. The characteristics of the return signal (amplitude, statistical variation, etc.) may provide some information regarding the target itself. The pulse repetition frequency (PRF) period or the time period between transmitted pulses determines the maximum

unambiguous range to which the radar can detect targets. Most radars operate over a large number of range settings (typically varying from around 0.25 up to 64 nautical miles) with the PRF period fixed by the combination of the maximum range setting and the particular pulse length utilized.

Figure 1 shows a simplified view of the basic radiation pattern. The vertical half power (or 3 decibel (db)) beamwidth (β) is usually about 15° to 20° wide to help compensate for the roll of the ship. The 3 db horizontal beamwidth determines the azimuth resolution (r_a) at any given range whereas the pulse length in units of distance defines the range resolution (r_r). The actual resolution cell area on the ocean surface may be approximated, in the case of marine radar, by the rectangular area, $r_a\ r_r$, or by the equation:

$$r_a\ r_r = Rc\tau \tan(\theta/2) \qquad (1)$$

where, R is the range,

c is the velocity of propagation of the electromagnetic waves,

τ is the pulse length, and,

θ is the horizontal beamwidth.

Figure 1 also shows the resolution cell geometry.

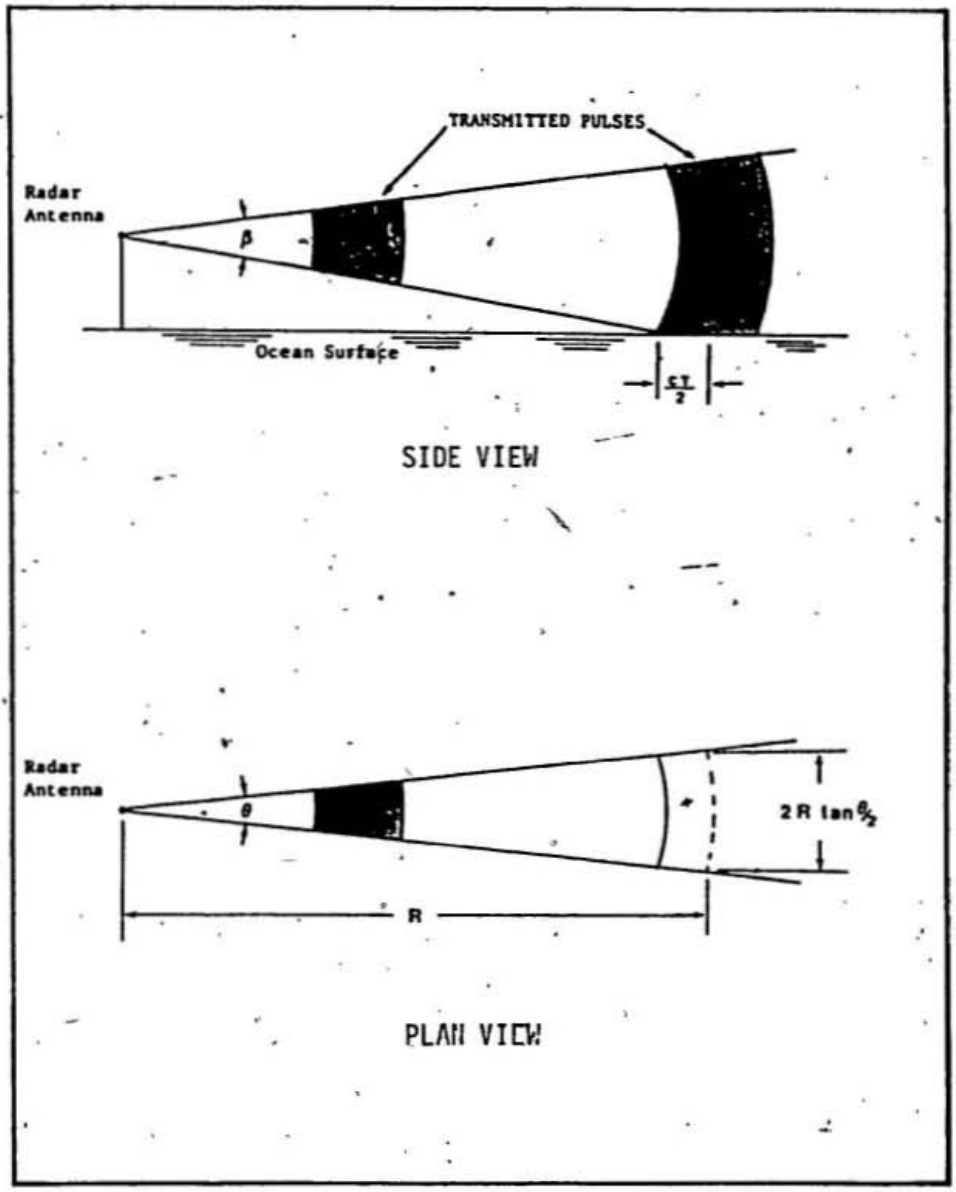

FIGURE 1 – PULSED MARINE RADAR TRANSMISSION – BASIC GEOMETRY

By mechanically rotating the (transmitting/receiving) antenna or electronically rotating the beam at a constant speed (usually around 20 to 30 revolutions per minute) while transmitting and receiving energy, a 360° view around a ship is obtained. Usually a number of PRF periods are exceeded before the antenna turns through θ so that the azimuth resolution is maintained. The returned energy is typically displayed on a cathode ray tube, commonly called a plan-position indicator (PPI) display. The PPI shows the returns from targets in polar co-ordinates.

Most marine radars operate with carrier frequencies (frequency within the transmitted pulse) in the S- and X-band regions of the electromagnetic spectrum. Usually they employ frequencies around 3 (S-band) and 9.5 (X-band) GHz, having wavelengths around 10 and 3.2 centimetres, respectively. Horizontal polarization is usually utilized, although circular polarization is also employed to provide improved performance when precipitation is present.

The ability to detect a target by radar is governed by the signal-to-clutter or the signal-to-noise ratio. Clutter is the unwanted signal returned from the area around a target, while noise is normally system noise generated within the radar. When the clutter is greater than the system noise level it is the limiting factor in detecting a target. If the clutter level is sufficiently high a target may go undetected. For marine radar, clutter

would be the return from the sea surface or precipitation. System noise is the limiting detection factor in the absence of clutter. In a standard radar receiver a signal-to-noise ratio of 10 db is typically required to provide a 50 percent probability of detection for a given target.

2.3 THE RADAR TRANSMISSION EQUATION

The radar transmission equation for a marine radar system in which the same antenna is used for both transmission and reception may be presented in the form (see, for example, Skolnik (1970)):

$$P_r = \frac{P_t G^2 \sigma \lambda^2 F^4}{(4\pi)^3 R^4 L} \qquad (2)$$

where, P_r is the received signal power,

P_t is the transmitted signal power,

G is the power gain of the antenna,

σ is the target radar cross section,

λ is the associated wavelength of the radar frequency,

F is the pattern propagation factor,

R is the antenna-to-target distance or range, and,

L is a summation of the system and atmospheric loss factors.

P_r and P_t are usually given in units of watts, while R, and λ are normally in units of metres, yards or feet. The radar cross section, σ, can have units of square metres, square yards, or square feet. The remaining terms are dimensionless.

The following subsections provide a more detailed description of the terms utilized in equation 2.

2.3.1 Transmitted and Received Power

The transmitted and received power can be defined a number of ways; for example, peak or average power may be used. The primary consideration is that the same form be used for both P_r and P_t. Peak transmitter power is normally used in the description of a particular radar system, and its value can easily range from 10 to 100 kilowatts.

2.3.2 Antenna Power Gain

The antenna power gain may be defined as the ratio of maximum radiation intensity from an antenna to the radiation intensity from an isotropic source (lossless) with the same power input (Skolnik, 1980). The power gain is related to the directionality of the antenna. The power gains of marine radar antennas are typically around 30 db relative to an isotropic source.

2.3.3 Radar Target Cross Section

The radar target cross section has units of area and may be defined as "the area intercepting that amount of radiated power which, when scattered isotropically, produces an echo equal to that received from the object" (Long, 1975). The radar cross section is a complicated function of the dielectric properties of the target at the particular frequency, its geometry, the angle of incidence and its surface conditions. In addition, it can depend on the particular polarization transmitted.

The normalized radar cross section, or backscatter coefficient, σ°, is the radar cross section per unit area of target irradiated surface and has a dimensionless coherent (or specular) and incoherent component. The coherent component is that obtained if the surface is smooth and amplitude and phase can be calculated fairly accurately mathematically. The incoherent component rises because of the presence of roughness. Its phase and amplitude are random and statistical modelling is usually required to predict its value (see, for example, Barrick (1970)).

2.3.4 Pattern Propagation Factor

The pattern propagation factor may be defined as the ratio of the electromagnetic field strength at a point in free space above a surface to that which would have been present if free space propagation applied in the absence of the surface and the point was in the radiated pattern maximum (Skolnik, 1970). Propagation over a smooth earth (or sea) results in reflection of both the transmitted and target reflected energy from the surface. The surface reflected energy causes destructive and constructive interference at the target and the antenna. Figure 2(a) illustrates the geometry involved for a smooth flat earth case and 2(b) demonstrates the variation in the propagation factor with range for a point target above a smooth flat earth. Figure 3 shows an alternate way of demonstrating the effect of the pattern propagation factor, illustrating that the antenna pattern is broken into a lobe structure. The expression shown in the figure gives the angle in radians which the lowest lobe makes with the surface when the radiated energy is transmitted horizontally over the surface. The expression also shows that for the same elevation the height of the lowest lobe is inversely proportional to frequency. Thus, higher frequency systems (X-band as opposed to S-band) in this situation should be able to detect low lying targets better.

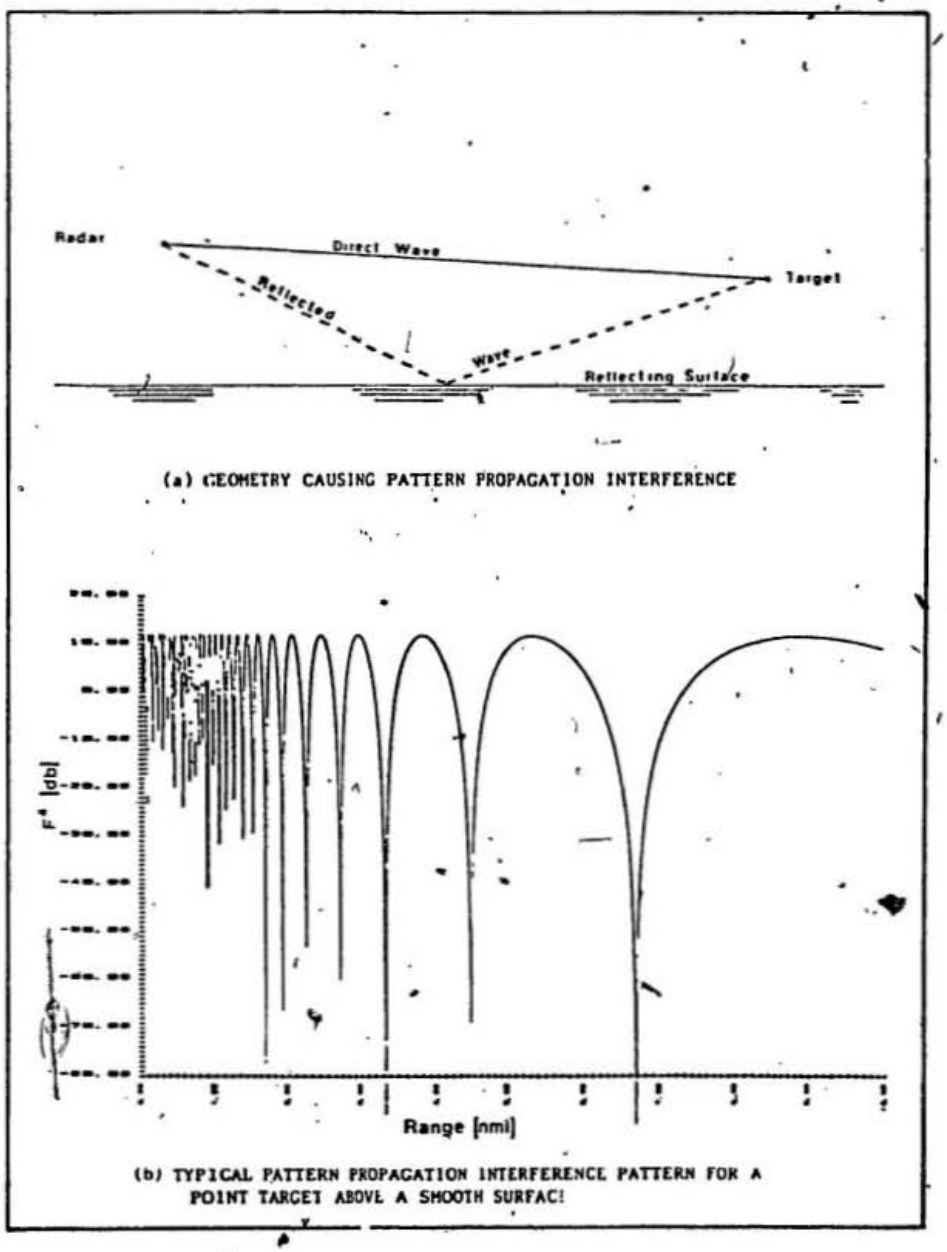

FIGURE 2 - GEOMETRY CAUSING PATTERN PROPAGATION INTERFERENCE AND TYPICAL INTERFERENCE PATTERN

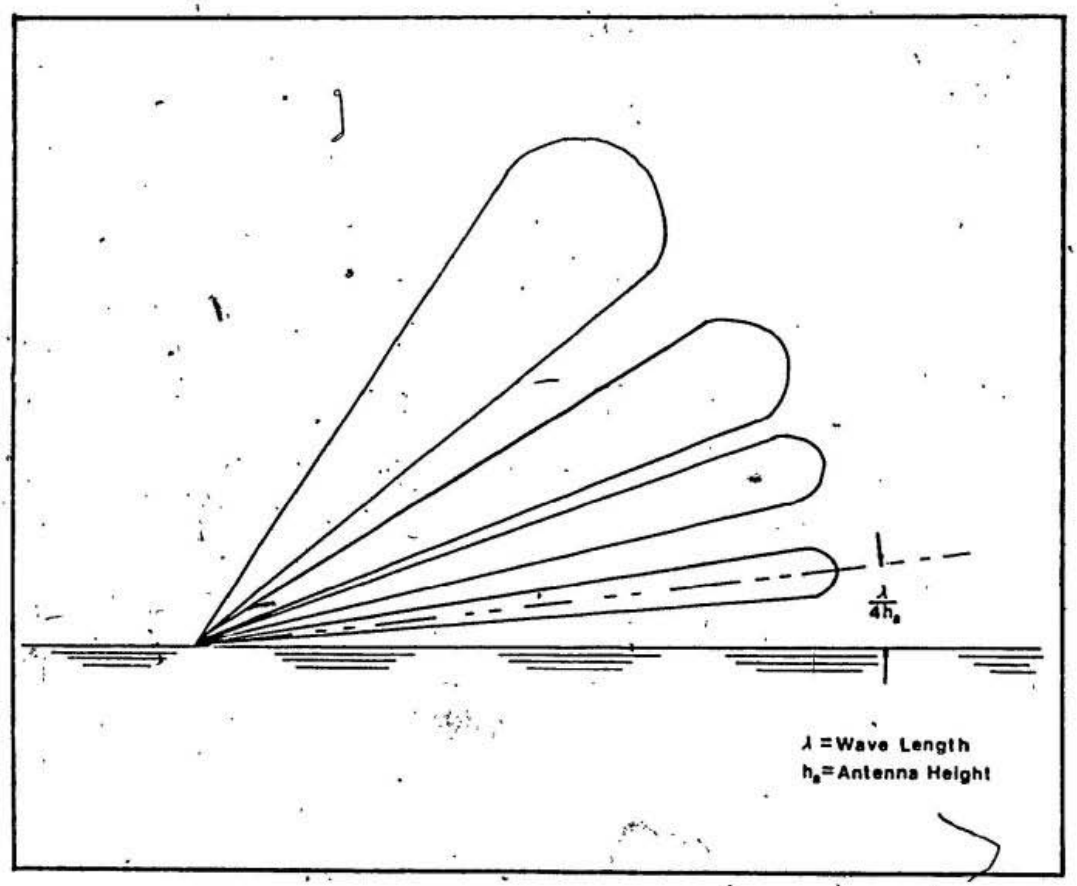

FIGURE 3 - RESULTANT EFFECT OF PATTERN PROPAGATION FACTOR ON ANTENNA PATTERN

The ocean surface is seldom perfectly smooth and the reflection off its surface (both forward and backward) is often considerably reduced. Also marine targets are usually vertically (and horizontally) extensive in their dimensions, resulting in an averaging effect on the pattern propagation factor. For these two reasons researchers often ignore this factor by setting its value to 1. Its effect however does show up in the received signal on occasion as illustrated in Figure 4.

2.3.5 Loss Factors

The losses include both system losses and those caused by the intervening atmosphere. If the measurement of the received and transmitted powers are not made at the antenna then the system losses will include waveguide, antenna, and duplexer losses. These usually vary with each particular installation but can be measured or calculated. For scanning radars an antenna pattern loss factor must also be included. The atmospheric loss is caused by the absorption of energy by the gas molecules. Normal atmospheric loss is very small over the range of operation of a marine radar (around 20 kilometres). The presence of fog and precipitation (rain, snow, etc.), depending on its concentration and type, can cause considerable attenuation.

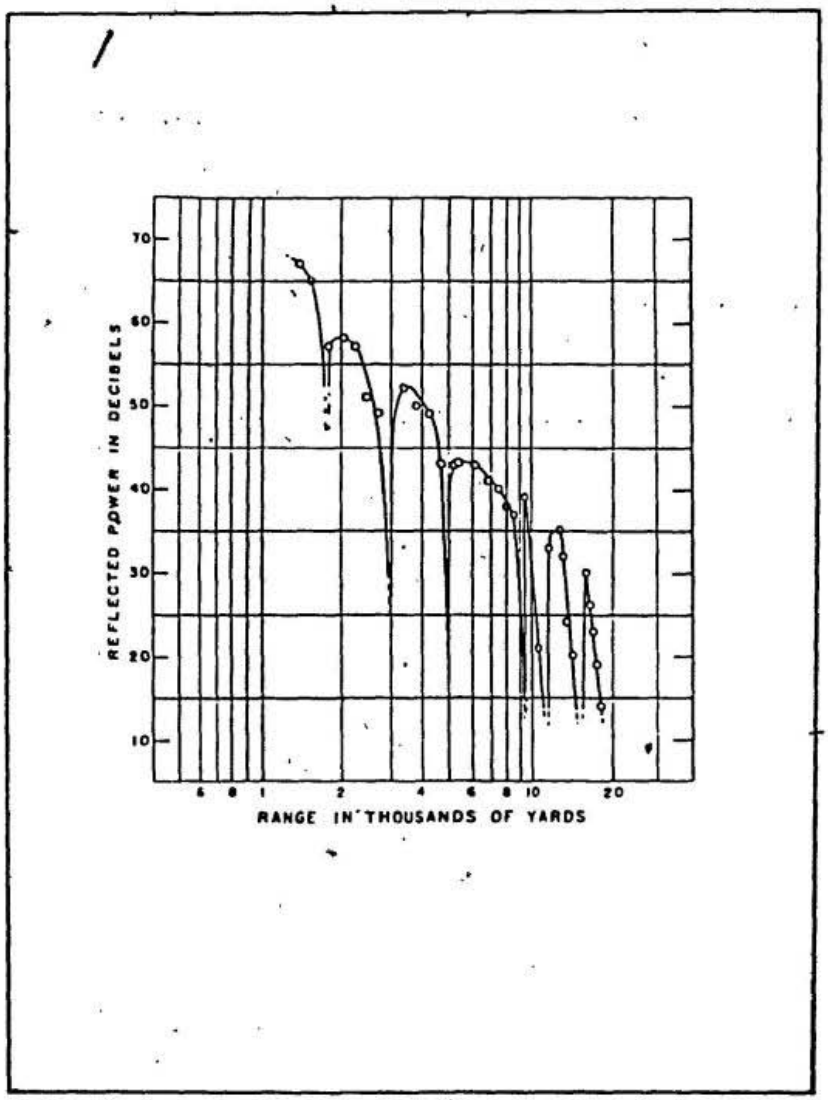

FIGURE 4 - PATTERN PROPAGATION FACTOR EFFECT ON AN ICEBERG RETURN AS OBSERVED BY BUDINGER (1960)

2.4 OTHER FACTORS AFFECTING DETECTION PERFORMANCE

2.4.1 Refraction

Refraction is the bending of the radar rays by the earth's atmosphere. The vertical index of refraction depends on the temperature, pressure and water vapor content of the atmosphere. Refraction may cause the radar horizon to be extended or reduced. Figure 5 illustrates these effects. Under standard atmospheric conditions the earth's radius seems to be effectively increased to 4/3 times the actual physical value (curve A, Figure 5) as far as radar ranges are concerned. This factor is reported to be between 6/5 and 4/3 in Arctic climates (Skolnik, 1980).

If the index of refraction were to increase rather than decrease with altitude then subrefraction will occur (curve B, Figure 5). This condition results in the radar being bent excessively upward, shortening the range of surface target detection.

Superrefraction occurs when the index of refraction decreases excessively with height causing the horizontal radar rays to propagate parallel to the earth's curvature (not shown in the Figure). This results in an infinite horizon distance (Blake, 1980). Such a ray is said to be "trapped".

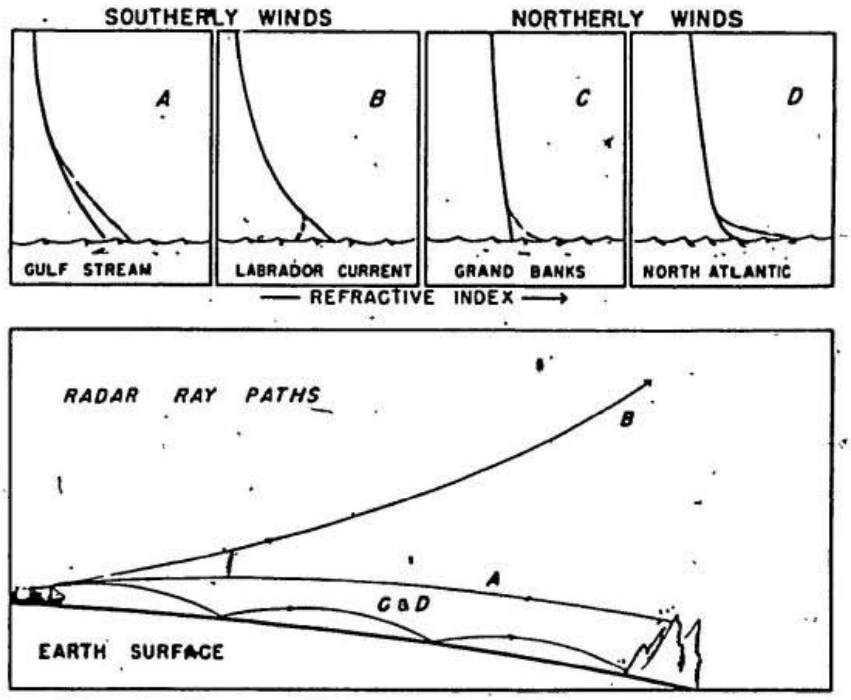

FIGURE 5 - ILLUSTRATION OF EFFECT OF REFRACTIVE INDEX VARIATIONS ON RADAR RAY PATHS (A - Normal; B - Subrefraction; C and D - Ducting) (Budinger, 1960)

Ducting occurs when the rays are bent downward with a greater curvature than that of the earth's surface (curves C and D, Figure 5). So called "evaporation ducts" exist over the ocean surface almost all the time, and in the North Atlantic the median value of the duct thickness is 10 metres in the summer and 30 metres in the winter (Skolnik, 1980). The occurrence of surface ducts will allow radars located in them to have rather increased ranges of detection beyond the radar horizon through the method of propagation, and because the spreading of the radiated energy will occur predominately only in the horizontal direction (the R term in Equation 2 will have a second as opposed to fourth power). If the radar is located above the duct it may not detect targets within the duct (such as growlers or bergy bits). The range information may be rather inaccurate for targets detected within a duct because of the propagation method. Also, when operating within a duct sea clutter will be displayed out to a much greater range because the attenuation caused by spreading will be reduced.

2.4.2 Diffraction

Diffraction causes radar rays to bend around the earth's surface just as light bends around corners. This phenomena is frequency sensitive and increases with increasing wavelength. The result is an extension of the radar horizon, although at standard marine radar

frequencies the increase is small. Because of diffraction S-band is often mistakenly thought to be preferable over X-band radar.

2.4.3 Sea Clutter

The radar return from the sea surface is called sea clutter. Its level and extent is dependent on the sea state. Nathanson (1969) undertook a detailed tabulation of sea clutter levels over a range of sea states, grazing angles (angles with respect to the horizontal) and frequencies for both horizontal and vertical polarization. The tabulation showed that the average normalized radar cross section of the sea surface increased with grazing angle, sea state and frequency. The normalized cross section seems to be greatest in the upwind direction (Long, 1975). Because the clutter is distributed over the surface, the average radar cross section per resolution cell is the product of the resolution cell area and the normalized radar cross section at that particular range (or, alternately, grazing angle). The actual radar cross section will vary widely, and detection of a target in clutter is highly dependent on the fluctuation statistics of the clutter and the target signal, as well as the overall amplitudes of the two.

2.4.4 Weather Clutter

The presence of meteorological particles resulting from fog, rain, snow or hail can cause a clutter problem as well. In general, lower frequency radars are not susceptible to these particles but these weather echoes can be quite strong at the higher frequencies (for example, at X-band frequencies). This type of clutter can mask a target just as sea clutter does. Unlike sea clutter, which starts at zero range and extends out almost omnidirectional from the radar antenna to a range determined by the sea state, weather clutter can occur in small localized portions of the area of coverage or it might cover the entire coverage area. Weather clutter is generally somewhat different from sea clutter in its statistical characteristics. Also, as it is a volumetric phenomena its radar cross section is determined by utilizing the volumetric resolution cell size at the particular range of interest.

2.5 DISCUSSION

The foregoing chapter shows that the detectability of a target by marine radar is dependent on a variety of system parameters and environmental factors. All of these factors can and have been mathematically defined in some manner. The only critical unknown factor as far as icebergs are concerned is the radar cross section. In

order to truly asses the performance of a given marine radar system for the detection of icebergs, a model of the normalized radar cross section then must first be derived. This can then be used to calculate the return from a given iceberg model.

CHAPTER 3

A REVIEW OF MARINE RADAR STUDIES OF ICEBERG DETECTION

3.1 INTRODUCTION

A number of significant studies have been undertaken over the last forty years regarding the assessment of iceberg detectability on marine radar. This chapter reviews the published research to date noting the pertinent results.

3.2 UNITED STATES COAST GUARD STUDIES

3.2.1 1945-46 Program

The first known major study of the detection of icebergs by shipborne marine radar appears to have been undertaken by the IIP in 1945 and 1946. The data was collected in the Grand Banks region. The original technical reports of this work are apparently no longer available (Hammond, 1982). Fortunately a detailed abridged report of the work, prepared by Budinger (1959), is still available.

The study employed both X- and S-band radar to measure actual signal return levels from icebergs as a function of range and aspect and to record the maximum

range of detection. Except for one particular test horizontal polarization was employed. Photographs of the icebergs were taken and, among others, measurements of the projected physical cross sectional area normal to the radar beam were made. Extensive and detailed meteorological and sea state measurements were also undertaken. In particular, measurements of vertical temperature and humidity profiles were made for the first forty feet of atmosphere above the sea surface to characterize the atmospheric propagation conditions. Finally, measurements of the signal levels of the sea clutter return and the maximum range to which it could be detected were compared with the sea state and wind conditions.

Iceberg radar cross sections were calculated from the 1946 data but a mix-up in the wavelengths provided erroneous results (Budinger, 1959 and Williams, 1979). No allowance was made for waveguide losses and a lack of knowledge regarding exact antenna gains and aperture areas also introduced errors in the results (Williams, 1979). An unexplained 15 to 17 db gain advantage of the S-band over the X-band system also adds some confusion (Budinger, 1959). Despite these sources of error some valuable results were obtained from these studies. These are discussed in the following paragraphs.

The maximum range of detection for almost all the icebergs fell well short of the distance to the radar horizon, although, both radars had very high peak transmitted powers. It was suggested that one reason this occured was the low reflectivity of the icebergs. Figure 6 shows the relationship found between the projected target area and the maximum range of detection for both frequencies. For both frequencies the range is shown to be, in general, directly proportional to around the fourth root of the projected physical cross-sectional area. The scatter in the points was said to be attributable to changes in meteorological (propagation) conditions, the difference in the proficiencies of the various operators, variations in the surface conditions of the icebergs and their dielectric properties, and varying sea conditions, which affected the roll of the ship (only the X-band system was stablized).

Figure 7 shows examples of the signal strength curves obtained. Although the absolute values are unusable the relative variation with range shows some important characteristics. There was considerable fluctuation in the signal levels but they do in general follow the $1/R^4$ (R being range) curve and exhibit the typical $1/R^4$ to $1/R^8$ transition zone, both of which are predictable by theory (pattern propagation factor effect) and often observed for ship targets. The transition zone, however, did occur at a much shorter range than that predicted for normal

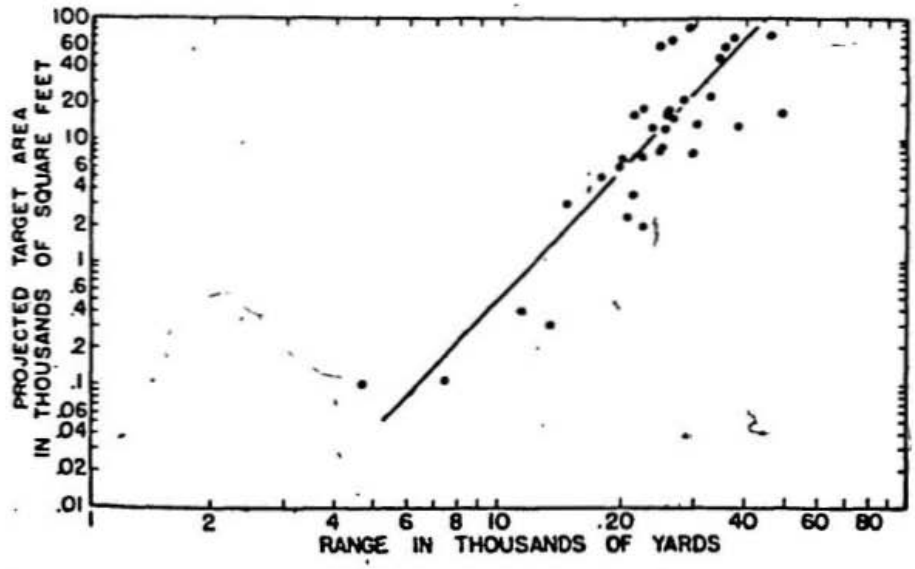

(a) X-band

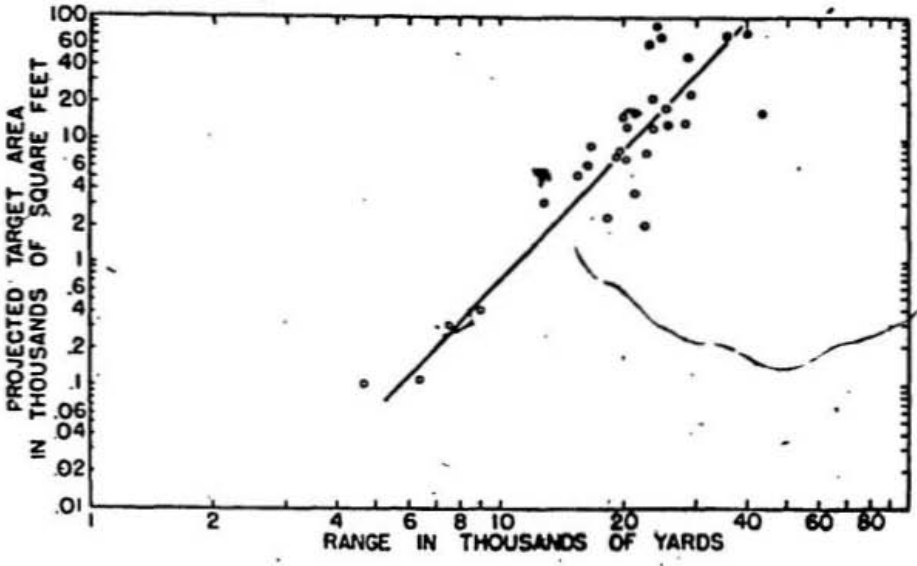

(b) S-band

FIGURE 6 - GRAPHS SHOWING MAXIMUM RANGE OF DETECTION AS A FUNCTION OF TARGET AREA PROJECTED ON A PLANE NORMAL TO THE RADAR (Budinger, 1959)

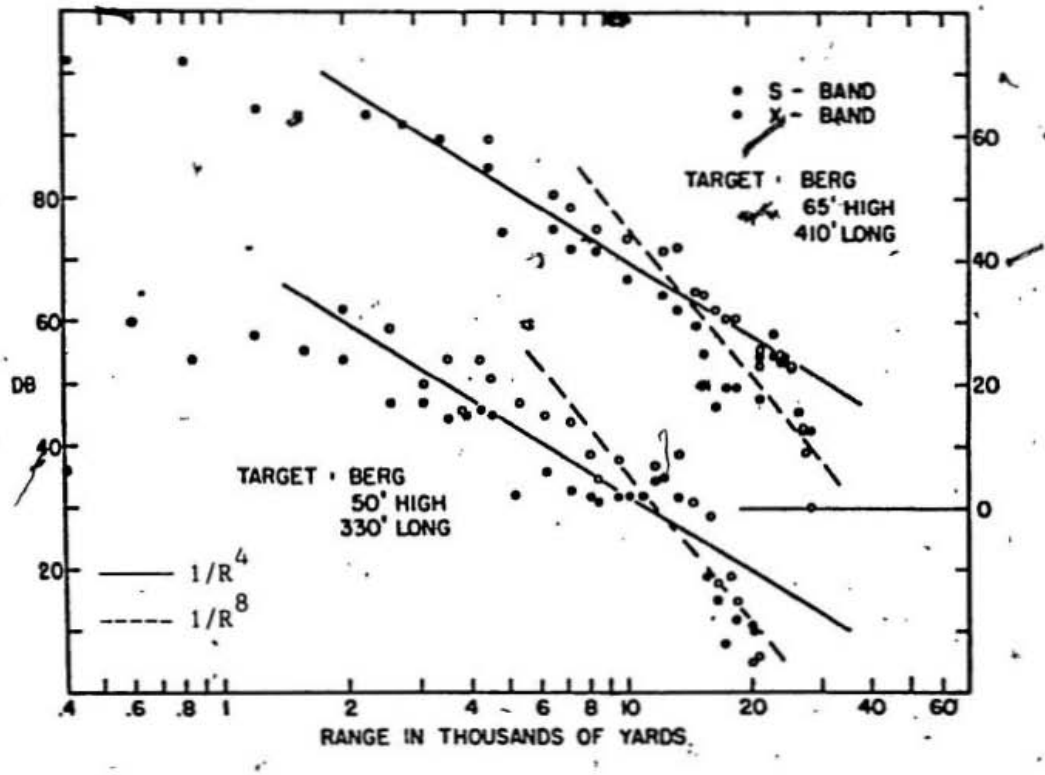

FIGURE 7 - EXAMPLES OF SIGNAL STRENGTH VERSUS RANGE CURVES OBTAINED IN USCG 1945/46 PROGRAM (Budinger, 1959))

propagation conditions. The range at which the zone occured also did not seem to vary consistently in proportion to the height of the target as it should have.

A comparison was made between the signal return from a ship and an iceberg. It was concluded from this and other observations that iceberg ice is a poor radar reflector. No quantitative results were given.

The effect of target aspect on signal return was also investigated but no relationship was established. It was concluded that although different aspects may give rise to widely varying signal strengths it appeared that measurements made from the moving ship resulted in the variations being random and unpredictable.

Comparisons between sea return and various ice targets indicated that the presence of clutter in high sea states may be the limiting factor in the detection of small ice targets within the clutter region. The S-band system seemed to provide improved detection capability in sea clutter. Vertical polarization was tested to determine if it would provide improved detection over horizontal polarization in sea clutter. No difference was detected.

Detailed observations of the meteorological conditions, correlated with target detection measurements, indicated that subnormal radar propagation conditions (and

attendant reduced ranges of detection) exist in times of poor visibility (fog) on the Grand Banks. This is a condition which is prevalent in that area.

3.2.2 1959 USCG Program

During thhe iceberg season off Newfoundland in 1959 the IIP launched another major study of the detection of icebergs by X-band (horizontal polarization) marine radar (Budinger, 1960). The radar data collection techniques used were very similar to those employed in the 1945/46 program. Again the meteorological conditions in the Grand Banks region were closely monitored and measurements of sea clutter levels made. A theoretical determination of the reflection coefficient of icebergs was undertaken and compared with a value derived from the data collected. Attempts were also made to correlate the variations in the received signal levels with the pattern propagation factor and the atmospheric conditions.

Figure 8 shows the resultant relationship between the actual physical iceberg cross sectional area normal to the radar and the maximum range of detection. The index of correlation is 0.81 and the standard deviation is $\pm$ 5,600 yards. The high value of the standard deviation is attributed to the use of data from a wide variety of sources. These included a large number of data samples obtained from merchant vessels and even some from the

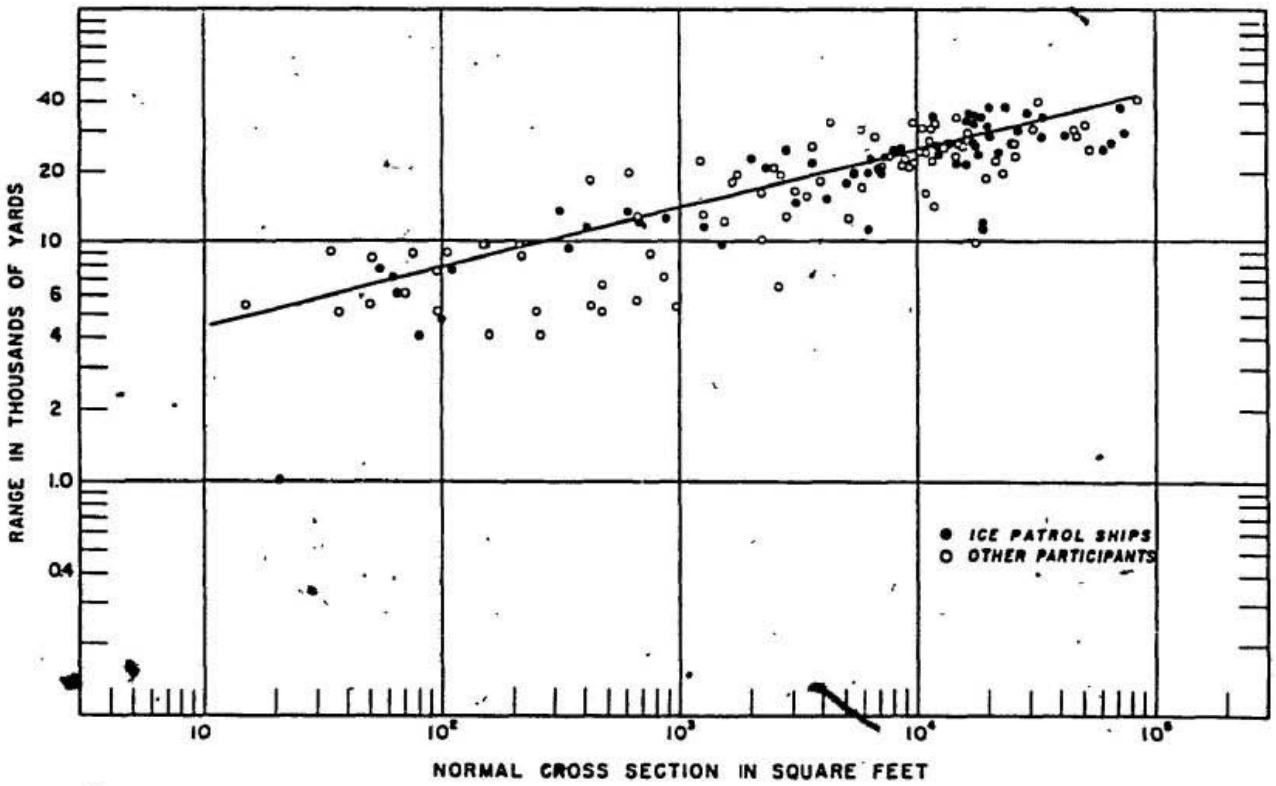

FIGURE 8 - MAXIMUM DETECTION RANGE VERSUS PROJECTED CROSS SECTIONAL AREA AS OBTAINED BY USCG IN 1959 (Budinger, 1960)

1945-46 program. Budinger cautions that the relationship might not be valid for growlers and that the range of detection for these may be less than that suggested by the figure.

A study of the signal fluctuations from a single iceberg at a constant range was undertaken. Over a four hour period the signal fluctuated by almost 10 decibels (db) and had a mean deviation of 1.9 db.

Budinger, using the theory that the average radar cross section of an aggregate of simple shapes in random orientation is one half the total physical cross sectional area, attempted to derive a reflection coefficient from his measurements. He observed that in the process of melting the surface of an iceberg takes on a pocked like [illegible]cromorphology which could be modelled by an aggregate of concave and convex curved surfaces having diameters greater than the X-band wavelength. Unfortunately an apparent mix-up in the calculations invalidates this work. Hammond (1982) suggested that this is a mix-up in wavelength as with the 1945-46 calculations, but the publication clearly states that only an X-band system was used in this work. Theoretical derivations by Budinger showed that the reflection coefficient of an iceberg with a water covered surface is 0.32 while a dry iceberg has a value of about 0.26.

A comparison was made between the reflectivity of ships and icebergs of equivalent sizes. The results indicated that icebergs are 59 to 62.5 times less reflective than ships.

The effect of iceberg aspect on detectability was also examined. Again, as in the previous program, no firm quantitative relationship was established.

An analysis of sea return, both theoretical and from actual measurements, indicated that growlers could be masked by sea clutter. This work also showed that theoretically the reflection coefficient of ice and sea water is virtually independent of frequency and that the relection coefficient of ice is three times less than that of sea water. Budinger reports that the frequency independence was confirmed by the 1945-46 studies. Because of the rapid decrease with incidence angle (up to about 60°) of the vertical polarization reflection coefficient for ice vertical polarization was considered inferior to horizontal polarization for iceberg detection.

After an analysis of the propagation conditions it was concluded that subnormal (subrefraction) propagation conditions prevailed in the Grand Banks region, particularly during the spring when icebergs and fog dominate. The results indicated, however, that no frequency preference exists at short ranges. The

attenuation in fog was considered insignificant when compared to other factors.

A comparison was made between theoretical fading and maximum detection range predictions and those which actually occurred on a particular iceberg. The correlation between the actual and theoretical results was poor.

Budinger finally concluded with a warning that radar, although an aid, cannot be relied upon to detect ice hazards in the North Atlantic.

3.3 DECCA RADAR COMPANY RESEARCH

3.3.1 Perry's 1952 Study

The first reported Decca Radar Company research into the detection of icebergs by marine radar was undertaken in the summer of 1952 (Perry, 1953). The study was conducted while Perry, an employee of Decca, travelled by ship on a return voyage from England to Port Churchill, Canada, through the Hudson Strait. During the passage Perry kept an extensive log describing the detection of a variety of ice targets on the ship's radar under a wide range of weather and sea conditions. Where possible detailed iceberg size and shape data were also recorded. No quantitative signal level measurements were made and only qualitative assessments of the signal strengths on

the radar screen were reported. Maximum detection ranges were logged.

Perry concluded that the detection ranges of icebergs were quite similar to those from land of about the same height. He also found that on all the icebergs, at every aspect there was some geometric feature that gave a substantial return. He felt that there were just as many facets on an iceberg as would be found on the face of a cliff. Finally, he concluded that the orientation of the wind direction relative to the location of a ship's radar and an iceberg has no effect on the quality of the echo received as far as it affects the atmospheric propagation conditions. He noted that, based on the sea and air temperature measurements made, conditions for subrefraction never existed.

Perry also made some very pertinent general observations regarding the minimum or shortest detection range of a variety of targets. The minimum detection range of land ice having hummocks and ridges was found to be 4 miles. Growlers and floebergs had a detection range in proportion to their size with the minimum detection range being 2 to 3 miles in a calm sea. Heavy swells or a rough sea was said to possibly cause excessive clutter and prevent detection of a growler or floeberg large enough to cause a disaster.

3.3.2 Research by Williams

In 1973 Williams published the results of a study on the detection of growlers by radar. The effects of varying a number of radar system parameters were examined.

Results of measurements comparing a high resolution (0.8^{o} horizontal beamwidth) with a low resolution (2.0^{o} horizontal beamwidth) X-band radar system using horizontal polarization showed that the lower resolution set was better for detection in high sea states under strong wind conditions, while the high resolution set provided longer range detection of growlers in pack ice under lower sea states and calmer wind conditions. In the high sea clutter conditions the low resolution set provided a much higher signal-to-clutter ratio. Williams stated that because the high resolution set was theoretically superior these results give the first evidence of the breakdown of sea clutter backscatter theory for very small resolution cell sizes.

The test results also suggested that for growler detection a multi-frequency radar system may be more effective than a single highly sophisticated single frequency radar. It was also pointed out that theoretically a S-band system does not radiate sufficient energy close enough to the sea surface to allow reliable detection of growlers, even at short ranges (as was

explained in Section 2.3.4).

Williams in 1979 published a historical review of ice detection at sea by radar. Using data from the 1945-46 IIP work he showed that the S-band radar system appeared to provide improved growler detection over an X-band system in high sea states (high clutter levels). Wide beamwidths were employed in both systems. Williams (1979) also developed a theoretical model of the radar cross section of a growler. In developing his model he made use of the theory that the median cross sectional values of irregular shaped objects can be approximated by their physical cross sectional area projected onto a plane orthogonal to a line joining the radar and the target. He noted that the peak value occurs infrequently. A spherically shaped model was used to approximate the growler as it was calculated to give the lowest radar cross section.

Using a peak value of 1 square metre or 0 dbsm (decibels relative to one square metre) for the model and reporting from earlier work on marine targets Williams stated that the peak radar cross section would exceed the mean by 10 decibels while the mean would exceed the median by another 10 decibels. Taking the reflection coefficient into account Williams concluded that -20 dbsm (median value) is a more appropriate value to employ for the cross section of a growler. Using this model he also determined

that a small iceberg will exhibit a radar cross section between 0 (median value) and 10 db (peak value).

Finally, Williams concluded that in order to detect growlers out to ranges of 1 to 5 nautical miles several radars and powerful anti-sea clutter processing is required.

3.4 BRITISH MINISTRY OF TRANSPORT STUDY

During the summer of 1952 the British Ministry of Transport in co-operation with Transport Canada and the National Research Council of Canada conducted a field program on a Canadian icebreaker to collect data on the radar detection of sea ice and icebergs using an X-band system employing horizontal polarization (Le Page and Milwright, 1953). The data was collected along the Labrador coast in the Hudson Strait and in Hudson Bay. The work included the measurement of the physical dimensions of the ice encountered, obtaining photographs of the iceberg shapes, meteorological measurements and measurements of the signal strength of target echoes.

A number of pertinent results were obtained. Initially, the authors reported that the measured vertical temperature profiles indicated that the conditions for subrefraction never existed. Occasionally temperature measurements did indicate that superrefraction conditions

might have existed. It was found that except for foggy or misty days every ice target was seen visually before it was detected on the radar. Subsequent calculations of the modified refractive index obtained when temperature and humidity data were considered adequate did show, however, that subrefractive conditions existed approximately 75 percent of the time. The magnitude of the sub-refraction was such that its effect would only be significant beyond about 3 miles. The possibility that certain wind directions relative to the location of iceberg and the ship might create sub-refractive conditions was examined and found to be unsubstantiated by the data.

The average maximum detection range for growlers was found to be 5000 to 6000 yards. Under rough seas (high clutter levels out to 3000 to 4000 yards) four growlers, seen visually, could not be detected, although they passed close to the ship. All had rounded surfaces and at least one was of sufficient size to inflict damage.

Large icebergs usually gave good strong echoes and were detected out to 20 miles. With the exception of the four growlers not detected all the ice formations that were sighted and approached within 2 miles of the ship were detected on the radar.

A plot of projected target area versus the range of detection at which the signal-to-noise ratio was 20 dB

(Figure 9) showed a definite relationship between the two. A least squares fit indicated a 3.2 power law relationship existed between them ((Range) $^{3.2}$ αA, the projected area). A comparison with the theoretical detection range of an equivalent sized metal sphere indicated that it is 60 to 70 times more reflective than the icebergs. It was noted that medium and large icebergs having sheer sides provided greater detection ranges than those with smooth rounded surfaces.

3.5 NATIONAL RESEARCH COUNCIL OF CANADA STUDIES

During the years 1953 to 1957 the National Research Council (NRC) of Canada carried out, on an annual basis, an extensive investigation of ice detection by marine radar (Hood, 1953, 1954, 1955, 1956, and 1958). The data collection took place during the shipping season in the Hudson Strait - Hudson Bay region. Both sea ice and iceberg targets were investigated. Data was collected through reports submitted by marine traffic equipped with commercial radars and transiting the area of interest. The information obtained included descriptions of the radar systems onboard the vessels, maximum ranges of detection for various ice targets, measurements of the sea clutter extent on the PPI display, observations of the detectability of targets in clutter, and measurements of the shapes and physical dimensions of targets, where possible. Although no frequency information was provided

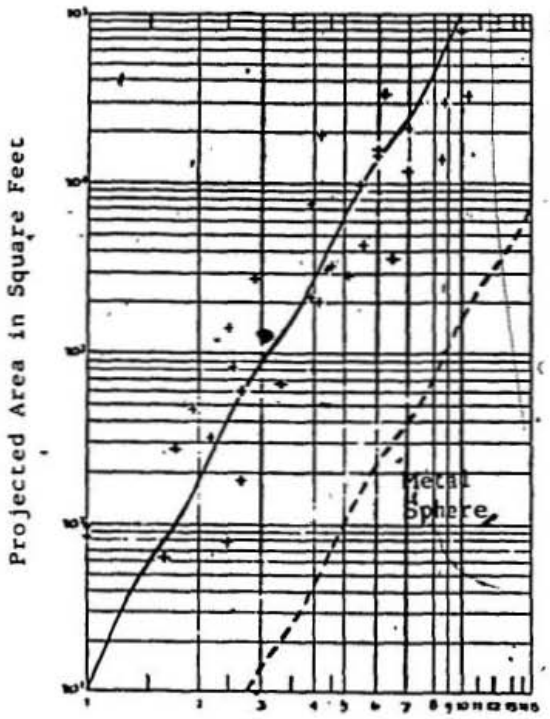

FIGURE 9 - PROJECTED ICEBERG AREA COMPARED WITH RANGE AT WHICH TARGET HAS ECHO STRENGTH OF 20db ABOVE NOISE (Le Page and Milwright, 1953)

it is assumed that most of the radars were X-band, as standard commercial radars usually operate at this frequency. It is also assumed that the polarization was horizontal. No quantitative signal level data was collected. The physical cross sections for the targets were derived by estimation from photographs and drawings. These were called the radar cross-sections in these reports.

Figure 10 shows the relationship found between the maximum detection range and the estimated radar cross sectional area which was given in the summary report (Hood, 1958). The solid line is the locus of the fourth power curve.

The scatter in the data is attributed to the many sources using radar systems having differing performance specifications and the requirement of having to estimate the cross section. It was stated that the detection range did fall within theoretical expectations. Growlers were given particular attention in the study. Of 54 growlers reported only 22 were detected by radar. All of those detected were outside the clutter region or in calm water. In several cases radar contact with growlers was reported to have been lost when they entered the clutter and none were reported as being detected in clutter.

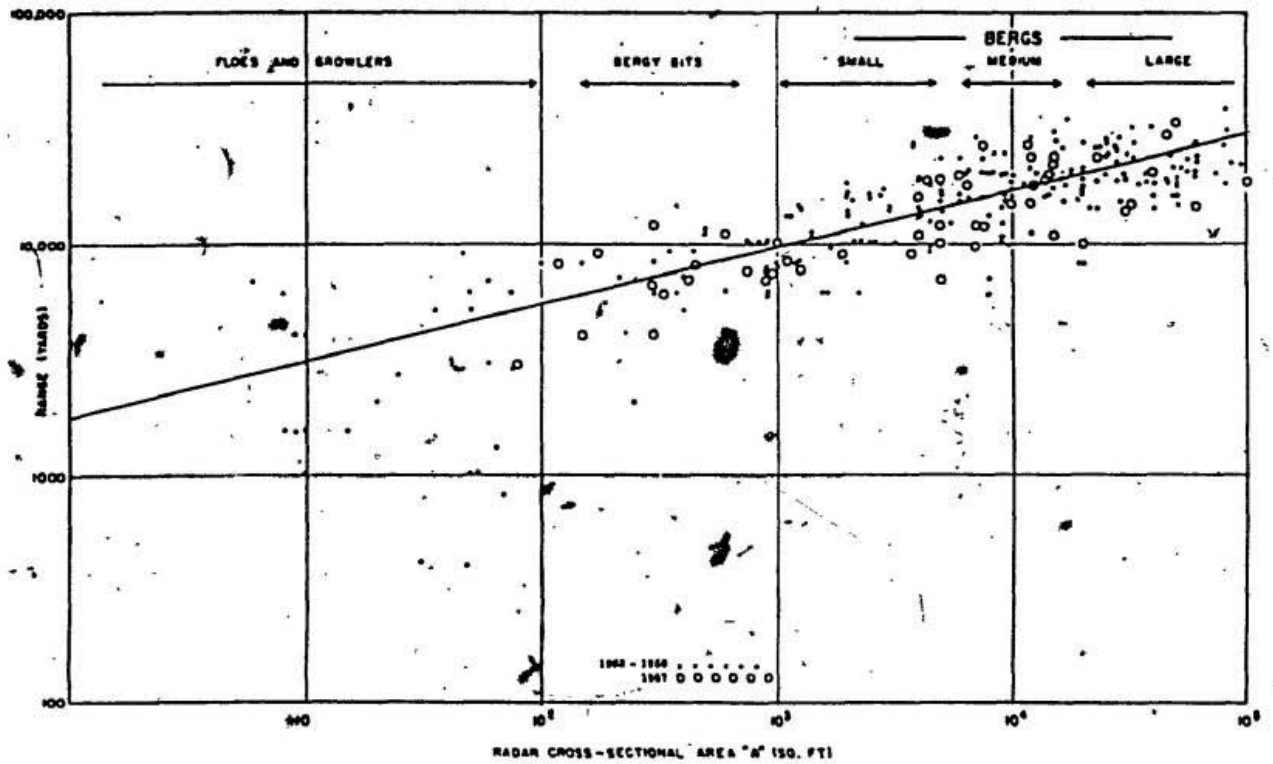

FIGURE 10 - MAXIMUM RANGE OF DETECTION VERSUS AREA OBTAINED BY NRC (Hood, 1958)

It was found that anomalous propagation conditions did occur in the area of investigation. The variations were, however, not considered sufficient to have any significant effect on the ranges of detection involved. It was also reported that no evidence was found to support the theory that radar ranges would be reduced considerably by pockets of cold air in the lee of an ice field.

The individual annual reports contained some important observations. Examining Figure 10 it is seen that there appears to be a saturating trend in the data points in the "large icebergs" area. Hood (1956) suggested that this was due to the radar horizon being reached and these icebergs are only detected when they were within the radar horizon. Being partially below the horizon they exhibited the sizes of smaller icebergs which were detected only at much shorter ranges. Figure 10 also shows very wide scatter in the "floes and growlers" area. It was also stated in the 1956 report that this is because the detection is occuring in sea clutter and that this type of detection analysis does not apply for these small targets (Budinger (1960) also suggested this).

3.6 OTHER STUDIES

Wylie (1968) discussed the detection of icebergs and growlers by radar in some detail. Although he provided no references for his information it is believed that his

information was derived from the results of other researchers. He attributed the variability of the radar echo from large icebergs to smooth flat faces which may or may not be oriented correctly towards the radar, depending on the particular aspect. It was suggested that sub-refraction and smooth sloping sides were the reason that icebergs are not detected at ranges that would be expected. Disappearing echoes were thought to be caused by either movement of the ship or rotation of the iceberg (which in turn presented a poor aspect to the radar). It was also stated that icebergs on the Grand Banks were 60 times less reflective than ships of equivalent echoing areas (a possible reference to the work of Budinger (1960)). A detection range varying from 3 to 15 nautical miles was given for icebergs. Wylie also stated that growlers were poor targets because of their size and shape. He noted that they are seldom detected at more than 4 nautical miles with 3 nautical miles being the expected maximum. Echoes from growlers were said to be almost impossible to detect when in a region of strong sea clutter, possibly because the growlers themselves are moved by the sea. Also, it was suggested that waves over 4 feet in height may render a growler undetectable.

In 1973 the Communications Research Centre (Canada) undertook a study involving the collection of X-band (horizontal polarization) marine radar data on icebergs for the Maritime Command (Cross and Lewis, 1973).

Quantitative data was collected while the ship was in transit between Halifax, Nova Scotia and Resolute Bay, Northwest Territories. Radar cross sections were calculated. Unfortunately, the only document published in the open literature did not provide any iceberg physical size information corresponding to the cross sections derived. Data were recorded from 18 iceberg targets ranging in size from large icebergs to growlers. The maximum range at which growlers could be detected was 4 to 6 nautical miles. One iceberg, whose closest approach to the ship was 14 nautical miles, was said to have a shape and smooth surface which might have caused it be a very weak and intermittent target.

During the years 1979 and 1980 Petro-Canada Exploration Limited, with the support of a number of other companies and the Canadian Government (Transport Development Centre), launched a major study into the development of a shipborne integrated ice hazard detection system (Jonasson et al, 1981 and Miller, 1982). The program involved an extensive theoretical evaluation of radar, sonar, and infrared detection systems; an extensive market survey; and a three month field program in which all the sensors were tested. A radar system which employed height, frequency, polarization and resolution diversity was utilized. Only samples of the data have been released to date. Figure 11 shows a plot of an iceberg X-band radar cross section versus range derived from the data

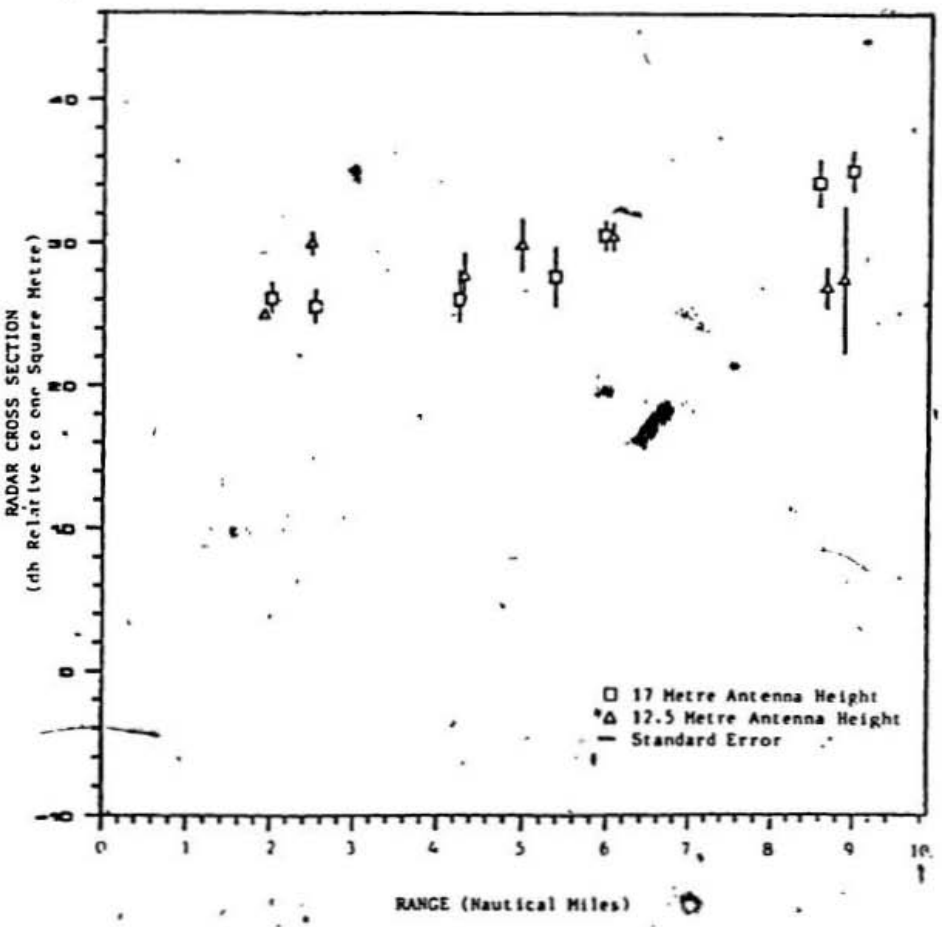

FIGURE 11 - MEASURED X-BAND (HORIZONTAL POLARIZATION) RADAR CROSS SECTIONS FOR MEDIUM BLOCKY ICEBERG (Miller, 1982)

collected.

Other than the size classification no other information was provided. Table 2 shows a summary of the detection capabilities obtained utilizing the entire system.

Pearson (1983) presented detection results obtained from a drill ship during Petro-Canada's exploratory drilling operations in the Labrador Sea and these are shown in Table 3. The lengths provided are the maximum waterline lengths. There is a slight error in the classification of the icebergs according to the lengths provided. The medium iceberg should actually be classed as a large iceberg and the small iceberg should be classed as medium.

Finally, Benedict and Hall (1979) undertook a similar study to that done by Petro-Canada, but stopped short of a field program. The work was undertaken for Transport Canada and an evaluation of radar, sonar, infrared and low light level television systems was made (Williams of the Decca Radar Company participated in the study and his publication in 1979 (described earlier) was a result of this work). The study examined in detail the atmospheric and sea state effects on marine radar. The emphasis was placed on growlers and the same spherical model as developed by Williams (1979) was used. In 1981 Lewis and

TABLE 2 - DETECTION RANGES FOR VARIOUS ICE TARGETS AS OBSERVED BY PETROCANADA (Miller, 1982)

TARGET	MINIMUM RANGE (nautical miles)	MAXIMUM RANGE (nautical miles)
GROWLER AND ICEFLOES	.5	1-2
SMALL ICEBERGS ($930\ M^2$)	2-3	3-5
MEDIUM ICEBERGS ($930 - 5574\ M^2$)	5	8
LARGE ICEBERGS ($5574 - 16,583\ M^2$)	12	12

(M - Metres)

TABLE 3 - MAXIMUM RANGES OF DETECTION ACHIEVED FROM A DRILLSHIP IN THE LABRADOR SEA (PEARSON, 1983)

TARGET	DETECTION RANGE (kilometres)
LARGE BERG (215M)	17 - 47
MEDIUM BERG (150M)	15 - 28
SMALL BERG (100M)	9 - 15
BERGY BIT (10M)	1 - 5
GROWLER (5M)	1 - 3

(number in brackets is waterline length in metres)

Benedict summarized the work of the Transport Canads study, noting that theoretically the instantaneous radar cross section of a growler can vary by as much as 40 db.

3.7 DISCUSSION

Almost all the research to date was undertaken using X-band radars and horizontal polarization. The results show some definite trends and characteristics in the detection of icebergs by marine radar. These concern the range of detection versus target size, the effect of aspect and shape, and the detection of growlers.

Figure 12 provides a summary of the range versus projected area curves obtained by the various researchers. The USCG 1945-46 results were included by Budinger (1960) in his 1959 results. The results of the Petro-Canada work is superimposed on the data as well. One half of the areas for each class (based on maximum length and height) supplied by Miller (1982) were used, with the small iceberg class assumed to covér the whole projected area range for that class and hence extended to do so. Table 1 was used to determine heights for Pearson's (1983) data by interpolation within the maximum length and height dimensions given for each class using the waterline length provided. Again, one half the areas obtained were utilized in the figure. This reduction to one half the area was employed because in examples given by Budinger (1960) and

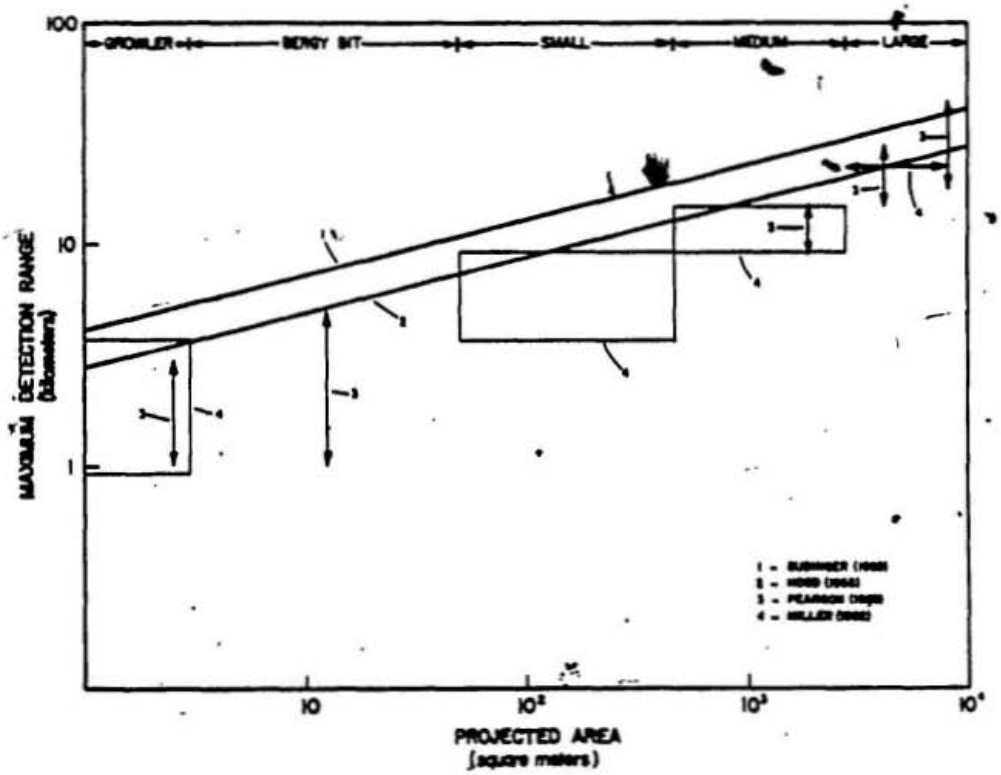

FIGURE 12 - SUMMARY OF X-BAND DETECTION CAPABILITIES OBTAINED THROUGH VARIOUS STUDIES

Hood (1954 and 1956) the actual projected area averaged about one half of the rectangular area defined by the maximum length and height of the icebergs. These curves show that there is a definite relationship between the range of detection and the projected area of the iceberg. The relationship can be described by the equation (which was used in Hood's studies and by Budinger):

$$R^4 = K A \qquad (3)$$

where, R is the range;

K is a constant dependent on the radar system performance characteristics; and,

A is the physical projected area of the iceberg normal to the radar.

The equation shows that the radar cross section is directly proportional to the projected area.

Scatter in the individual data sets can be easily explained by the use of radars having differing K values, variations in propagation conditions, the pattern propagation factor, etc. The K factor however indicates the performance level of the radar. Note that the K factor of the USCG 1959 military radar system outperformed all the radars used by Hood and Petro-Canada's radar systems except for the larger icebergs. This indicates that commercial radars have still not achieved the performance

capabilities of military radars in use 20 years ago.

The studies were unable to demonstrate (except theoretically) any relationship between the aspect and detectability of an iceberg. This suggests that the aspect or the shape of the iceberg directed towards the radar may not be a primary factor. Rather the actual projected area is more important. Examples presented of icebergs having smooth sloping sides giving weak returns indicate that there is some incidence angle dependence for the radar cross section.

Two independent studies provided similar results on the reflectivity of icebergs (Le Page and Milwright, 1953 and Budinger, 1960). They suggest that icebergs are around 60 times less reflective than ships or spherical metal targets.

Limited tests comparing two frequencies indicated that S-band radars gave improved detection capability in sea clutter. Both horizontal and vertical polarizations gave the same results in clutter. All the studies show that the primary factor limiting the detection of growlers is the presence of sea clutter. Sea clutter signal return levels may not be the only cause of detection problems. The height of the waves may be high enough to physically obscure the growler as well.

Finally, although theoretical values for the radar cross section (Williams, 1979) and the reflection coefficient (Ibid. and Budinger, 1960) of an iceberg were derived, neither have been verified by the data collected. The lack of a known normalized radar cross section model seriously inhibits the assessment of marine radars for the detection of icebergs.

CHAPTER 4

DERIVATION OF A NORMALIZED RADAR CROSS SECTION MODEL

4.1 INTRODUCTION

Photographs, sketches and descriptions by a number of researchers (see for example, Perry 1953 and Budinger, 1960) show that on a macroscale (dimensions very much larger than a microwave wavelength) icebergs can have surfaces ranging from very smooth flat or gently curving types to those consisting of many facets (each also much larger than a microwave wavelength) having a cliff like appearance, and any combination in between. Also, as pointed out by Budinger (1960) the overall shape and surface morphology of icebergs varies widely from one to another with no two being exactly alike. The derivation of the exact radar cross section for an individual iceberg would then be extremely difficult and meaningless on a general scale. Therefore it would seem more productive to derive a normalized radar cross-section model for one of the relatively smooth areas of an iceberg and utilize it along with physical iceberg models to determine expected radar cross sections.

The approach taken here is then the determination of a suitable normalized radar cross section model of a planar surface which is essentially the washed and eroded

relatively smooth surface of a piece of glacial ice. This is considered typical of the facets of the surfaces of icebergs found in the Northwest Atlantic.

4.2 IDENTIFICATION OF AN APPLICABLE THEORETICAL MODEL

Budinger (1960) was the only researcher found providing detailed information on the microscale features of an iceberg surface. As pointed out in Chapter 3 he described the microstructure as an aggregate of concave and convex surfaces. It was also suggested that the spheres, of which the individual concave or convex shapes would form a portion, could easily have diameters greater than 3.2 centimetres (an X-band wavelength). Although no indications were given as to the overall vertical roughness, it can be assumed (not unrealistically) much less than this value. Therefore the surface could be described, on the microscale, as a smoothly rolling type with vertical excursions being small on a wavelength scale.

Barrick (1970) and Long (1975) described and showed examples of a statistical model for deriving the average incoherent backscatter (average incoherent normalized radar cross section). The model is based on an original rigorous mathematical treatment of scattering formulated by Rice (1951, as reported by Barrick, 1970, and Long, 1975). Peak (1959) expanded on this work to compute the

average normalized radar cross section (as reported by Barrick, 1970, and Long, 1975). The model uses a perturbation technique as opposed to the physical optics approach (Barrick, 1970). Although the model was originally developed for nonmagnetic homogeneous material it was expanded by Barrick and Peake (1967, as reported by Long, 1974) for applications to materials having any value of relative permeability.

The model proposed expresses the surface or the scattering target as an extended roughened plane with the excursions from the mean slope being described mathematically as a random process (Axline and Mater, 1974). It requires that the surface height roughness spatial autocorrelation function be known for the surface. The normalized correlation function or the correlation coefficient (autocorrelation function divided by the mean square height) is actually used in the mathematical formulation. A term similar to the Fresnel zone reflection coefficient is also employed.

In absolute terms the model does not necessarily give correct values, but on a relative basis the variation of the average incoherent normalized radar cross section with incidence angle, frequency and polarization fitted extremely well with actual measurements for natural surfaces. Both Barrick (1970) and Long (1975) also stated that a strong specular backscatter component should

theoretically be added to the model at near vertical incidence angles. This would cause a substantial increase in the normalized radar cross section at these angles. However, based on results presented by Barrick (1970) for an asphalt surface at an X-band frequency the incoherent scattering component model, on a relative basis, followed the shape of the measured data curve quite well even at near vertical incidence angles.

To determine whether the model is applicable here, at least theoretically, the restrictions on the model must be compared with a physical description of the surface. One general criterion for the applicability of this type of model is that the overall surface area (A) be very large compared to the square of the wavelength (λ), or $\lambda^2 \ll A$. At X-band frequencies (λ approximately 3.0 centimetres) this criterion is assumed to be easily met. The restrictions on the slightly rough surface statistical model as described by Barrick (1970) are:

1) $kh < 1.0$

2) $\partial S/\partial x,\ \partial S/\partial y < 1.0$

3) $\langle (\partial S/\partial x)^2 \rangle = \langle (\partial S/\partial y)^2 \rangle$

where, k is $2\pi/\lambda$, the free space wave number;

h is the root mean square height of the surface roughness;

λ is the radar wavelength;

S is the mean square surface height roughness ($< s^2 (x,y) > = h^2$ (<> means average)) and,

x,y are orthogonal directions on a plane through the mean height of the planar rough surface.

The first restriction is that the surface roughness height must be small. The second requires that the surface slopes be relatively small. And the third restriction signifies that the roughness must be isotropic.

4.3 PHYSICAL APPLICABILITY OF THE MODEL

This section compares the description of the glacial surface under consideration with the physical restrictions on the model. The following discussions are based on comparisons with X-band radar wavelengths. From Budinger's (1960) description of the surface microstructure (Section 4.2) the overall vertical roughness could be assumed to be much less than 3.2 centimetres. In other words the surface can be assumed to have vertical excursions satisfying the first restriction, that is, $kh < 1.0$.

Barrick (1970) stated that a natural surface that is smoothly curving and has roughness radii of curvature large compared to the radar frequency limit will satisfy the second restriction that the surface slopes be relatively small. Budinger's description of the surface having a concave and convex structure would seem to

indicate that this restriction is also satisfied.

It is intuitively obvious that the surface roughness is isotropic. Thus, the third restriction is considered satisfied.

It is concluded then that the surface under consideration can be said to meet the physical restrictions imposed in order to enable utilization of the incoherent scattering model proposed here.

Barrick (1970) gave two variations of the model. One version uses a Gaussian form of the surface height correlation coefficient while the other employs an exponential form. Mathematically these are:

$$\rho(r) = e^{-r^2/\ell^2}$$

for the Gaussian form, and,

$$\rho(r) = e^{-|r|/\ell}$$

for the exponential form, where r is a measure of the separation between any two points on the surface, and ℓ is the correlation length. The correlation length is usually the separation distance at which the autocorrelation function reduces to e^{-1} of the value of r = 0 (see, for example, Axline and Mater, 1974).

Barrick (1970) also stated that surfaces having a Gaussian surface height correlation coefficient are smoothly curving with derivatives at all points, while those possessing an exponential form are jagged and have many vertical facets. The Gaussian version, based on the glacial surface microstructure description, seems to be applicable here.

4.4 MATHEMATICAL DESCRIPTION OF THE MODEL

Using a Gaussian height correlation coefficient the mathematical equations providing the average incoherent σ° for vertical (V) and horizontal (H) polarization are (Barrick, 1970):

$$\sigma^\circ_V = \left| \frac{(\varepsilon_r - 1)\left[(\varepsilon_r - 1)\sin^2\theta + \varepsilon_r \mu_r\right] - \varepsilon_r^2 (\mu_r - 1)}{\left[\varepsilon_r \cos\theta + \sqrt{\varepsilon_r \mu_r - \sin^2\theta}\right]^2} \right|^2 \qquad (4)$$

$$\times\ 4 k^4 h^2 \ell^2 \cos^4(\theta) \exp(-k^2 \ell^2 \sin^2\theta)$$

$$\sigma^\circ_H = \left| \frac{(\mu_r - 1)\left[(\mu_r - 1)\sin^2\theta + \varepsilon_r \mu_r\right] - \mu_r^2 (\varepsilon_r - 1)}{\left[\mu_r \cos\theta + \sqrt{\varepsilon_r \mu_r - \sin^2\theta}\right]^2} \right|^2 \qquad (5)$$

$$\times\ 4 k^4 h^2 \ell^2 \cos^4(\theta) \exp(-k^2 \ell^2 \sin^2\theta)$$

where k, h, and ℓ are as before,

θ is the incidence angle in degrees with respect to the vertical;

μ_r is the relative permeability of the surface; and,

ε_r is the relative permittivity of the surface.

Ice, being a non-magnetic material, has a permeability of one. It has been found that pure ice has a dielectric constant (real part of the complex permittivity) of 3.17 $\pm$ 0.7 for frequencies greater than 1 MHZ (Evans, 1965). An investigation of the dielectric properties of glacial ice (REMOTEC Applications Inc., 1982) showed that a value of 3.2 seems appropriate for glacial ice at 120 MHz. Loss tangent (ratio of the imaginary part to the real part of the complex permittivity) values have been reported to be 7×10^{-4} (Williams, 1979) and 5×10^{-5} (Benedict and Hall, 1979) at frequencies around 10 GHz. Using a value of 3.2 for the real part, the loss tangent corresponds to values ranging from 1.6×10^{-4} to 2.24×10^{-3} for the imaginary part. The values are very small and are considered negligible for calculation purposes. Using values of 3.2 for ε_r and 1 for μ_r equations (6) and (7) can now be written for glacial ice in the form:

$$\sigma_V^\circ = \left| \frac{4.84 \sin^2\theta + 7.04}{\left[3.2 \cos\theta + \sqrt{3.2 - \sin^2\theta}\right]^2} \right|^2 \qquad (6)$$

$$\times 4 k^4 h^2 l^2 \cos^4(\theta) \exp(-k^2 l^2 \sin^2\theta)$$

$$\sigma_H = \left| \frac{2.2}{\left[\cos\theta + \sqrt{3.2 - \sin^2\theta}\right]^2} \right|^2 \qquad (7)$$

$$\times\ 4\,k^4\,h^2\,l^2\cos^4(\theta)\exp(-k^2\,l^2\sin^2\theta)$$

4.5 DISCUSSION

A model has been proposed for the determination of σ° for an eroded and washed relatively smooth planar glacial surface. Even though a mathematical formulation has been derived it is not possible to apply the model without access to suitable measured data. The following chapter deals with this aspect.

CHAPTER 5

VERIFICATION OF THE MODEL

5.1 INTRODUCTION

The lack of information regarding the actual roughness parameters, for the glacial surface under consideration makes it impossible to apply the model practically. One way to overcome this problem is to empirically fit the model to actual measured normalized radar cross sectional values. There have been, however, no suitable data found in the marine radar research studies undertaken to date.

Another source of data that can be used are airborne scatterometer results. The following sections provide a description of these data and deal with the empirical fitting of the model to the results.

5.2 DESCRIPTION OF THE DATA

Gray et al (1981) and Gray (1983a) presented σ° data from a number of icebergs obtained using an airborne K_u-band (13.3 GHz) radar scatterometer. The data were collected in April of 1980 from a number of icebergs which were situated in frozen sea ice in Melville Bay. Figure 13 summarizes the results. They show a 10 to 15 decibel

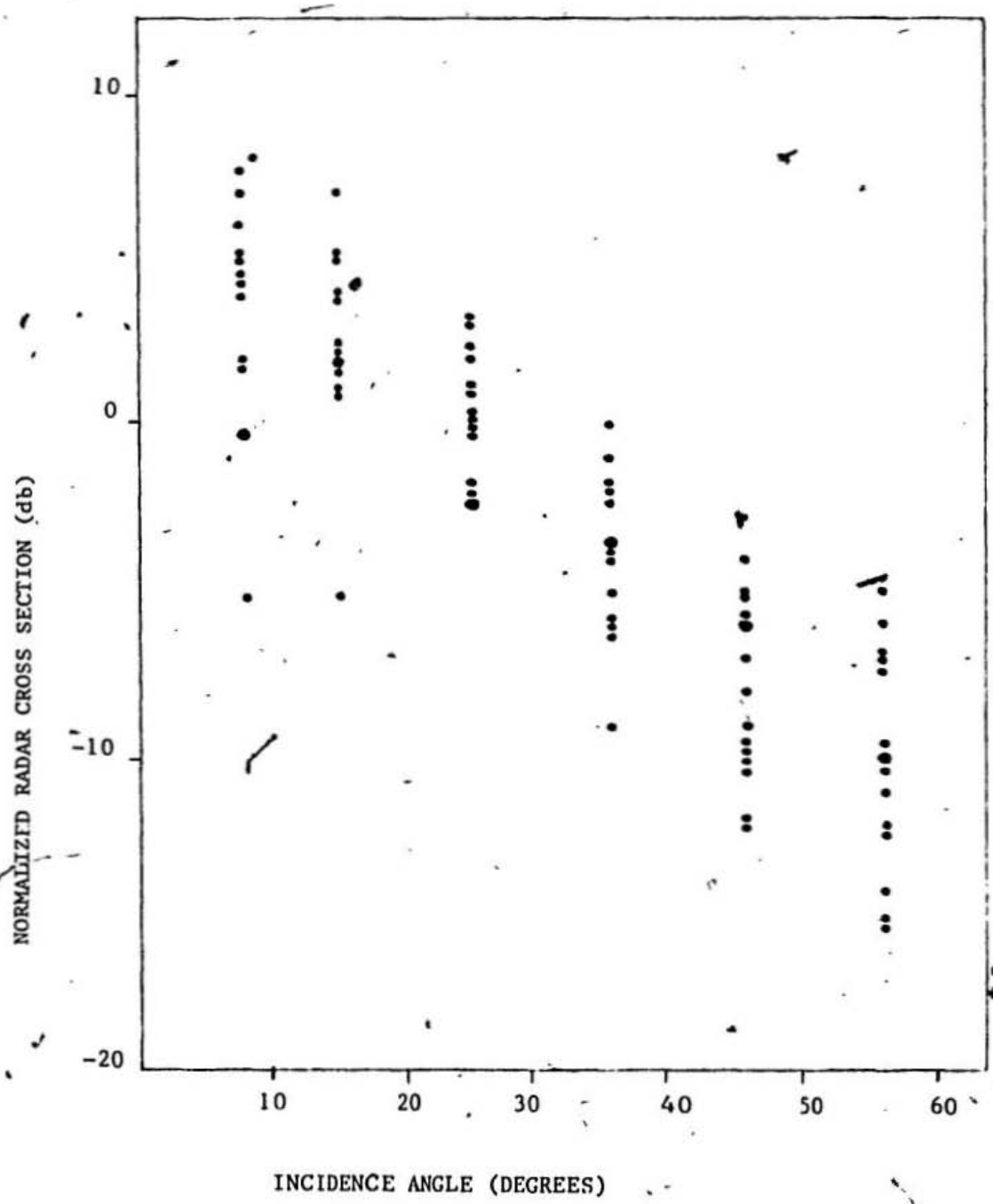

FIGURE 13 - NORMALIZED RADAR CROSS SECTION VALUES OBTAINED FOR ICEBERGS LOCATED IN FROZEN SEA ICE (GRAY, 1983a)

variation at any incidence angle from the vertical over the range of measured angles. This agrees well with the fluctuations obtained by researchers using marine radars (see Chapter 3).

Unfortunately there are a number of shortcomings in this data set which preclude it from being used to verify the model. There was no information collected regarding the actual local incidence angle on the surface of the icebergs. In fact, the one author of the group who actually selected the data points chose the maximum value for each iceberg at every incidence angle (Gray, 1983b). Also, there was no information regarding a description of the surface of the iceberg. However, the same author agrees that the icebergs, being essentially in winter conditions in frozen sea ice, would not have washed and eroded surfaces representative of those for which the theoretical model would be applicable. Finally, because the shape of the iceberg was not provded it is unknown whether the actual area resolved was flat and equivalent to that of the scatterometer footprint or areal resolution cell (20 metres X 20 metres). This would create errors in the actual calculation of σ°.

In 1978 normalized radar cross sectional data for icebergs were collected using the same scatterometer (Gray et al, 1979). Figure 14 shows the resultant σ° for two icebergs at various incidence angles. The data were

• Points used in Figure 15

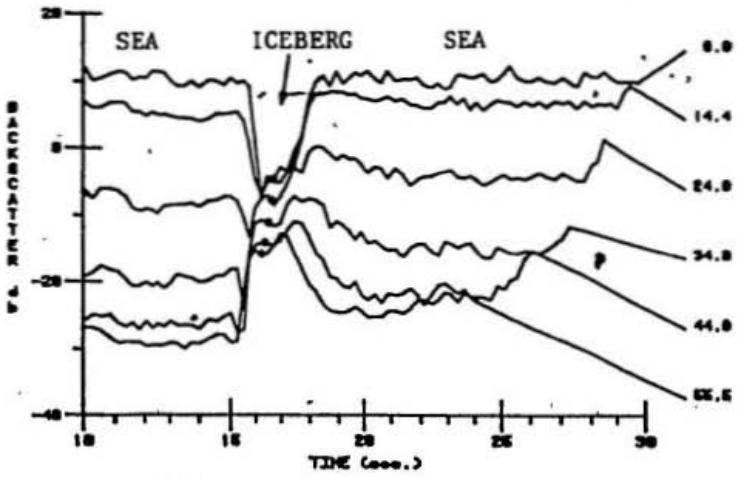

(a) Scatterometer VV output from larger berg as a function of time for different (aft) incidence angles.

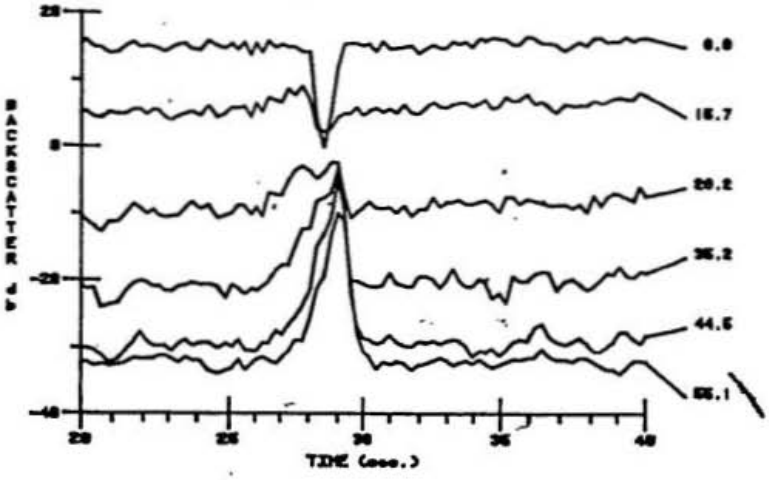

(b) Scatterometer HH output from smaller berg as a function of time for different (aft) incidence angles.

FIGURE 14 - NORMALIZED RADAR CROSS SECTION FOR TWO ICEBERGS OBTAINED USING A 13.3 GHZ SCATTEROMETER (VV-vertical polarization, HH-horizontal polarization) (Gray et al, 1979)

obtained in September under open water conditions off Baffin Island. The larger iceberg was tabular like in appearance in that its upper surface was flat, at least on the macroscale. Although, Gray (1983b) suggests that it was probably not a tabular iceberg in accordance with the WMO classification system. The smaller iceberg was of an irregular shape and was classified as being pinnacled. The curves shown also demonstrate that the amplitude of the sea surface normalized cross section can be greater than, equal to, or less than that of an iceberg, depending on the sea state and the incidence angle.

The uncertainty regarding the exact incidence angle and the actual surface geometry of the smaller iceberg makes it practically impossible to use this data. However, the surface of the larger iceberg was relatively flat and indicated by Gray (1983b) to be slightly rough and washed so that it would represent a surface for which the model would apply. Also, the scatterometer footprint was much smaller than the surface area, assuring an accurate measurement of σ_v°.

The incidence angle data shown in Figure 14 were calculated by obtaining σ_v° over ten degree intervals, averaging the values and labelling the resultant value with the average incidence angle within the given interval. Therefore, it is assumed that the normalized cross section data for this iceberg are adequate for the

purpose of empirically fitting the model.

5.3 RESULTS

Figure 15 is a plot of σ°_{v} versus incidence angle for the larger iceberg. The points were derived from Figure 14(a). The data shown in Figure 15 are for vertical polarization at 13.3 GHz (2.25 centimetre wavelength) and the model is first applied to this data directly.

The parameters k, h and ℓ in equations (8) and (9) are unknown. However h only effects the amplitude, which is already known from the data, and only the product, $k\ell$, is required. Therefore, a curve can be empirically fitted to the data by trial and error using different values of $k\ell$ and fitting the curve shape to that of the data (Detailed calculations are provided in the Appendix). Following this procedure it was found that a value of $k\ell = 2.1$ gave a good curve fit to the data as shown in Figure 16. A Chi-square test confirms the goodness of fit (see Appendix).

It is suggested then that the model can be fitted to this data. The resultant value of ℓ, the correlation length is 0.75 and it was indicated by Gray (1983b) that this was a reasonable correlation length. It now remains to extrapolate down to X-band frequencies and horizontal polarization.

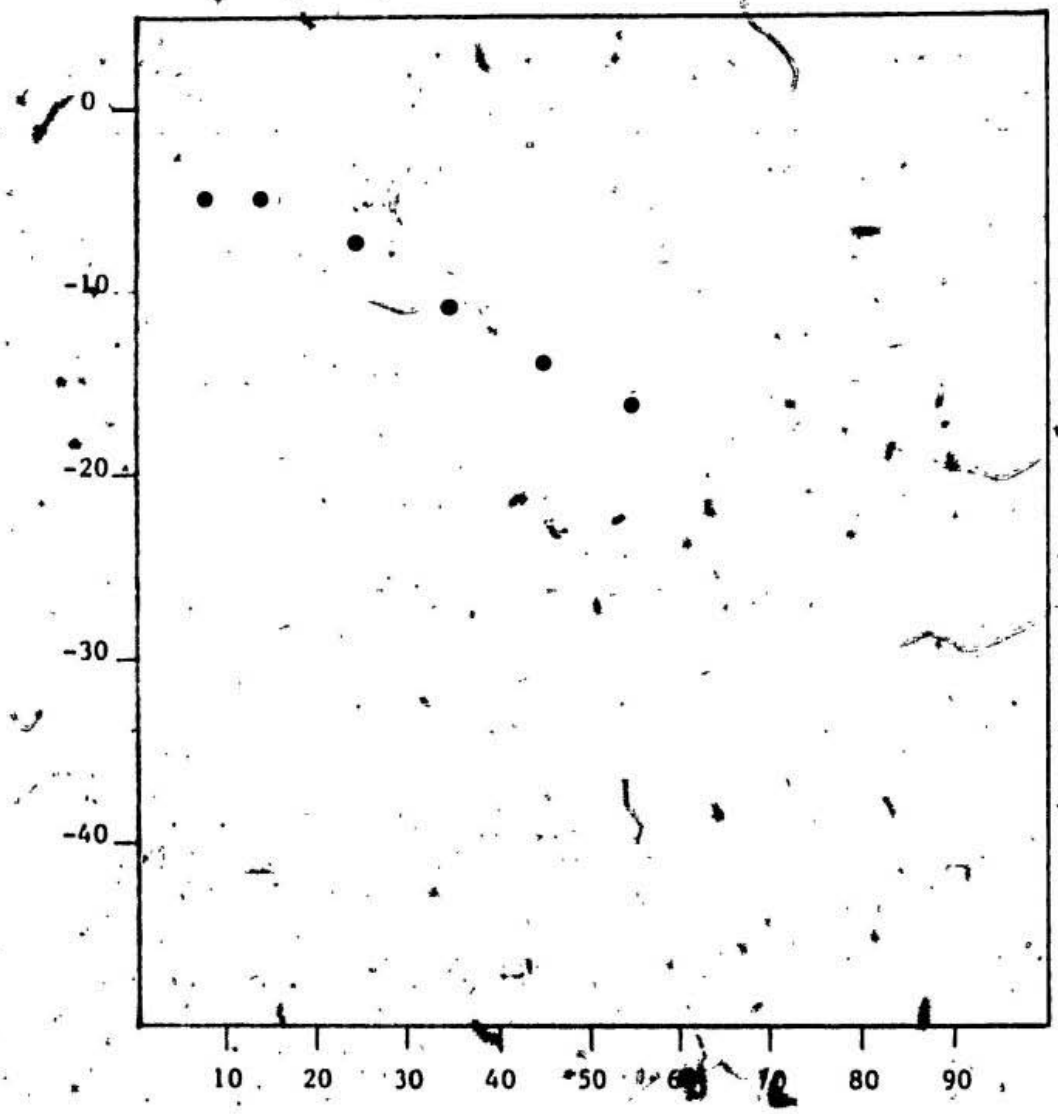

FIGURE 15 - PLOT OF NORMALIZED RADAR CROSS SECTION VERSUS INCIDENCE ANGLE FOR AN ICEBERG SURFACE

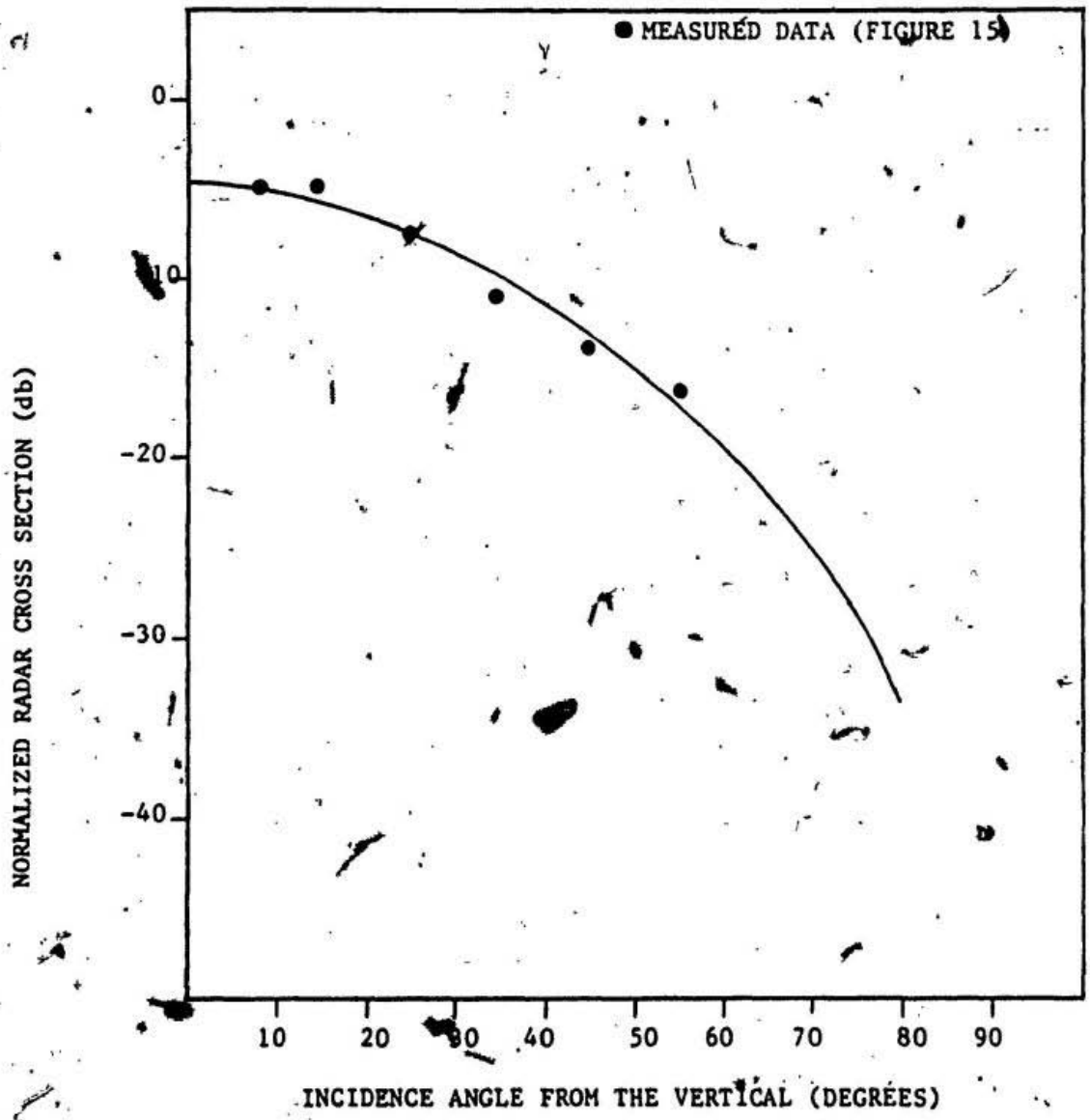

FIGURE 16 - APPLICATION OF SLIGHTLY ROUGH SURFACE MODEL TO 13.3 GHZ (VERTICAL POLARIZATION) ICEBERG DATA

Examination of equations (6) and (7) shows that for both horizontal and vertical polarizations at vertical incidence the σ° values are equal. Also, at vertical incidence the only difference caused by frequency is the K factor, which is known for both frequencies (2.79 at 13.3 GHz and 1.96 at a 9.5 GHz (3.2 centimetre wavelength) X-band frequency). The ℓ value is independent of frequency and has already been determined. Therefore the $k\ell$ value at 9.5 GHz is 1.48. The value, h, is still unknown, but is also independent of frequency and does not require determination.

To perform the actual extrapolation it is only necessary to determine the value at vertical incidence (0°) and derive the remainder of the σ° values relative to this. The difference between the k^4 value at both frequencies is 6.12 decibels (10 log k^4 (at 13.3 GHz) - 10 log k^4 (at 9.5 GHz)) with the 9.5 GHz value being lower. Thus, the first value for 9.5 GHz at 0° is 6.12 decibels down from that at 13.3 GHz. Ignoring the h factor (setting it equal to one) the remainder of the curve is calculated relative to this first value. Figure 17 shows the resultant curves for both horizontal and vertical polarization. The detailed calculations are given in the Appendix.

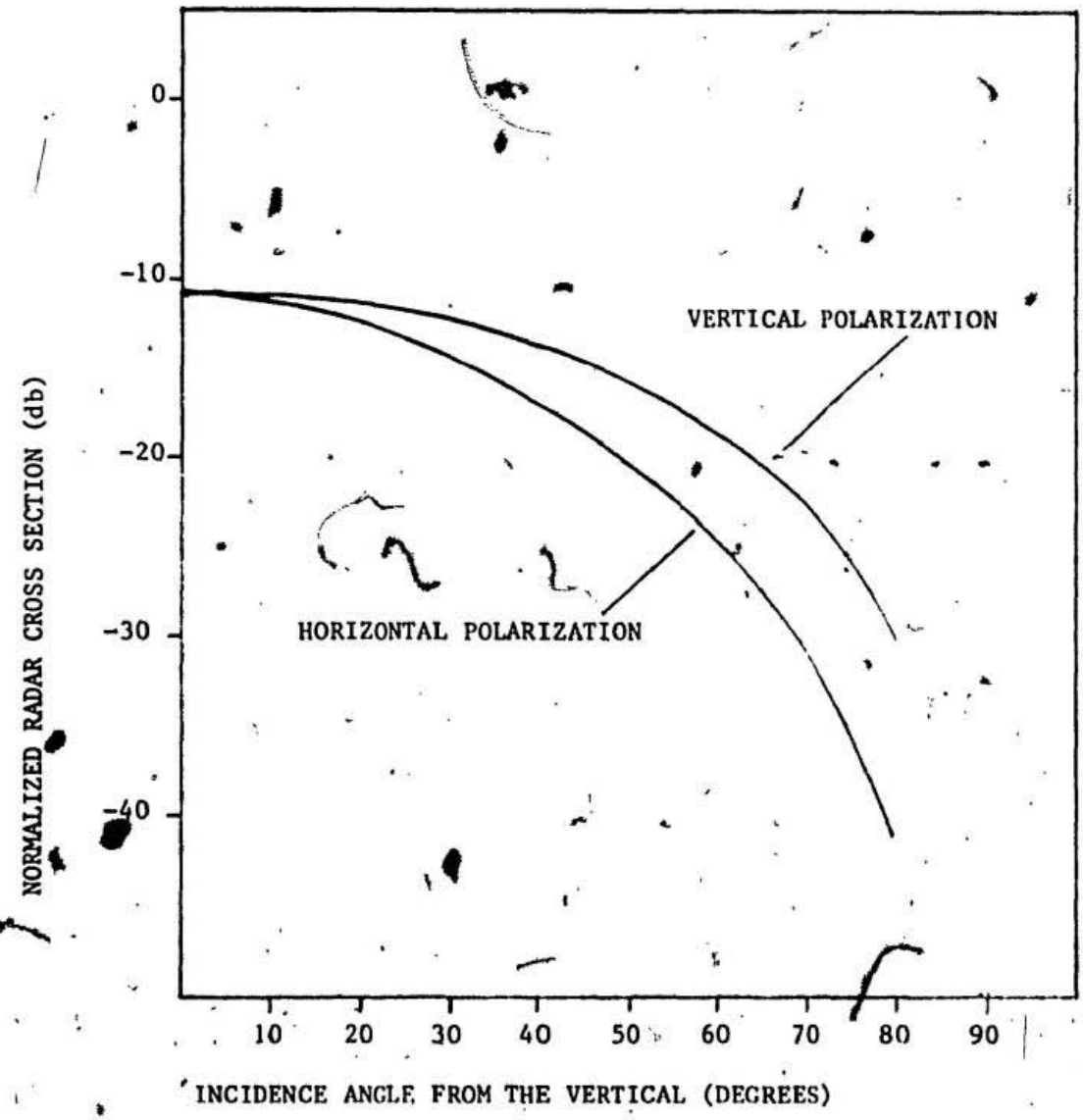

FIGURE 17 - APPLICATION OF SLIGHTLY ROUGH SURFACE MODEL TO AN ICEBERG SURFACE AT 9.5 GHZ THROUGH EXTRAPOLATION FROM 13.3 GHZ.

5.4 DISCUSSION

By empirical fitting to a limited data set and extrapolation down to the frequency of interest a model has been derived. It is now necessary to examine the validity of the model. This is extremely difficult because of the lack of suitable data. However, by making some basic assumptions it is possible to check the model against some limited data.

Crispin and Siegel (1968) stated that for complex targets in which the components contributing to the radar cross section can be said to add incoherently (that is, the phases of the component cross-sections are randomly distributed) then the average total cross section of the target can be estimated by simply adding the amplitudes of the cross sections from the various components. As icebergs can in general be classified as a complex target this methodology should be applicable to these as well. Alternately, on the average an iceberg face can be considered to be composed of a number of facets having a wide range of surface areas and orientations possessing random like characteristics. It should be possible then to approximate the average iceberg face by one surface having a single slope and area which is the average of those for all the facets. The radar cross section would then be the value for this single face. As was shown in Chapter 3 the radar cross section of an iceberg is directly proportional

to the projected area. Therefore, the σ° value for the face would be the value for the surface having the slope obtained through the averaging process. To determine the average σ° value for icebergs it is necessary to obtain an estimate of the average slope of an iceberg face.

Table 1 shows length and height ranges for the various sizes of icebergs. Using these values it is possible to obtain some idea of the range of slopes possible. The limits (with the exception of tabular icebergs) are found to be at least 4.6 metres high by 121.9 metres long (medium iceberg) to 77.7 metres high by 121.9 metres long (large iceberg). These correspond to average overall slopes which could range from about 7° to 33°. For tabular icebergs the slopes of the sides will approach 90°. Therefore it is reasonable to expect marine radar incidence angles ranging from close to 0° to almost 90°. Considering the random nature of the iceberg shape it should also be reasonable to assume that the average slope would be around 45°. From the model (Figure 16) this predicts an average σ°_{H} value of about -18.5 decibels.

On the basis of the data collected by Le Page and Milwright (1953) they determined that the X-band (horizontal polarization) radar return from an iceberg was on the average 60 to 70 times less than that of an equivalent sized metal sphere. The normalized radar cross section of a large perfectly conducting metal sphere

(having a radius much greater than the wavelength) is 1.0. Making use of the result that the radar cross section of an iceberg is directly proportional to its area then from this comparison the average σ_H° value for an iceberg is between 1/60 and 1/70 or -17.8 decibels to -18.5 decibels. These values agree extremely well with the average value of -18.5 decibels derived from the model using an estimated average slope of 45°.

Le Page and Milwright (1953) also found that the actual values ranged from about 400 to 30 times less than that of a metal sphere, or, alternately, they had values ranging from -26 decibels to -15 decibels. Using the model this range corresponds to slopes varying from just over 30° to slightly over 60° the mid-range value of which is slightly over 45°.

Budinger (1960) determined from two measurements at X-band (horizontal polarization) that icebergs were between 62.5 and 59 times less reflective than equivalent sized (projected area) ship targets. The latter value was obtained when that ship was stern on to the radar. Assuming that the stern can be approximated by a large metal sphere the same logic can be used here as with the observations of Le Page and Milwright to give a σ_H° value of 1/59 or -17.7 decibels. Again this value agrees quite well with the value derived from the model for an average situation.

The data presented by Miller (1981) for an X-band radar (horizontal polarization) and shown in Figure 12 gives another opportunity to compare the model with measured data. No dimensional information was provided but the iceberg was classed as medium blocky, and, from the figure, it was detected out to the maximum range for its class (see Table 2). This indicates that it was in the maximum size range for this class. The area of the side of the iceberg, estimated roughly by multiplying the maximum height and length dimensions together (150 feet (45.7 metres) and 400 feet (121.9 metres), respectively, from Table 1), is 5574 square metres or 37.5 dbsm (decibels relative to one square metre). This class of iceberg is characterized by steep precipitous sides, the slopes of which would probably be considerably greater than the average 45° value. Assuming as before that the face of the iceberg can be represented by one large slightly rough surface applicable to the model, and also assuming a slope between 60° and 90° (corresponding to incidence angles of 30 and 0°, respectively), σ_H° values of about -14 to -11 decibels would be obtained (Figure 17). Combining these with the surface area estimate gives a range of cross section values for the iceberg of 23.5 to 26.5 decibels relative to one square metre. From Figure 11 it is seen that the bulk of the values range from about 24 to 30 decibels relative to one square metre. Considering the approximations the estimates would seem to fit the measured values very well.

A number of researchers have reported or observed fluctuations in the order of 10 decibels or greater in the return power from an iceberg at a given range. The model indicates that a $\pm$ 15° variation around 45° will give about a 10.5 decibel variation in σ_H°. It is reasonable to expect that the combined variations caused by the roll of a ship and the iceberg, along with the slow rotation of an iceberg (changing the aspect) could cause a variation equivalent to this. In other words the predicted variations of σ_H° with incidence angle agrees reasonably well with fluctuations in actual measurements.

Figure 12 showed that the maximum range of detection and, in turn, the radar cross section of an iceberg is in general directly proportional to the total projected area. This suggests that overall shape (domed, pinnacled, blocky, etc.) is a secondary factor, although geometrically it will have some effect on the total projected area. This would help explain why direct observations were unable to establish any relationship between the radar return and aspect. The model and the physical description of an iceberg surface (on the macroscale) provided indicates that the return from an iceberg will be dependent on the incidence angles to the various facets and the total areas of the individual facets making up the surface. This also then is in agreement in general with Figure 12 and suggests that overall shape is not necessarily the dominant factor.

From Figure 18 it is seen that the model predicts that, at least for frequencies between 9.5 and 13.3 GHz, σ° increases with frequency over the majority of the incidence angles. It also predicts that vertical polariztion will give higher σ° values over most of the incidence angle range as well. However, it is well known that sea return increases with frequency and is usually higher for vertical polarization (at least at low to moderate sea states). Therefore, in a situation where clutter limits detection, the advantage of using a higher frequency or vertical polarization may be negated. Budinger (1960) indicated that from actual measurements no improvement was found in detection of an iceberg in clutter using vertical polarization. Unfortunately there appears to be no data available to check the actual frequency or polarization variations given in the model. It is noted however that for horizontal polarization and angles beyond 50° there is a cross over. Also, at 45° (determined earlier as the slope of the average iceberg) there is only slight over 2 decibels in the difference at the two frequencies. This would suggest that on the average only a slight increase might be expected in σ° by increasing the frequency within the range examined.

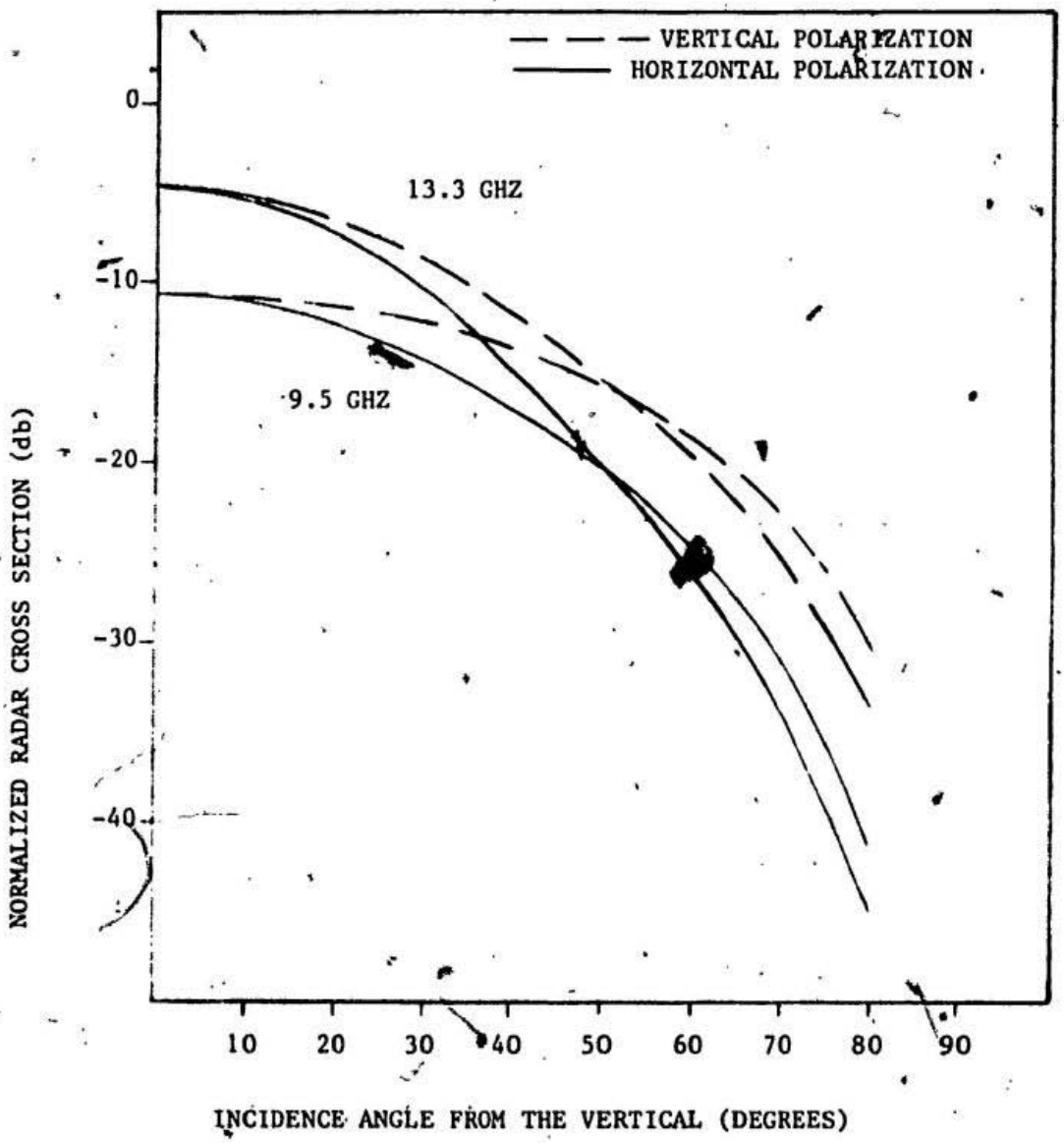

FIGURE 18 - FREQUENCY AND POLARIZATION COMPARISON USING SLIGHTLY ROUGH SURFACE MODEL

CHAPTER 6

CONCLUSIONS

The need for a quantitative assessment of the detectability of icebergs on marine radar has been clearly demonstrated. A review of the factors affecting the detection of by targets by marine radar shows that the one unknown factor which severely limits the ability to undertake such an assessment is the radar cross section of an iceberg.

Past research studies (with results available in the public domain) on the assessment of marine radar have either not addressed the problem of determining the radar cross section or have been unable to derive values verified by actual measurements. The exception to this are data released for one iceberg from one otherwise confidential study (Miller, 1982).

A comprehensive review of the research to date does provide some important insights into the problems regarding iceberg detection. The presence of sea clutter severely limits the detectability of icebergs, especially growlers and bergy bits at short ranges. In general icebergs are poor radar reflectors having cross sections on the average in the order of 60 times less than metal

spheres projecting an equivalent sized area normal to the radar.

The range of detection of an iceberg is shown to be dependent on its projected physical cross sectional area which is in turn directly proportional to the range raised to the forth power. Considerable spread exists in the data, however. Comparison of detection ranges for various radar systems indicates that commercial marine radars in operation today have not achieved the detection capabilities of military marine radars in operation 24 years ago, at least as far as maximum detection range is concerned. Finally, researchers were unable to establish any relationship between aspect and iceberg detectability.

From physical descriptions it has been shown that the average iceberg can be described as a very complex target. Those frequenting the Northwest Atlantic and expected to be encountered by offshore platforms and marine traffic are shown to have washed and eroded surfaces. On the microscale the surface is slightly rough and smoothly rolling. A slightly rough surface statistical model for the average incoherent normalized radar cross section using a Gaussian form of the surface height correlation coefficient was shown to be applicable to the surface on a physical basis. Using empirical fitting to a limited data set at 13.3 GHZ (airborne scatterometer data over a large relatively flat iceberg surface) and extrapolating to 9.5

GHZ this model has been adopted to determine the normalized radar cross section of a slightly rough washed and eroded glacial (iceberg) surface. The validity of the model has been verified using some general assumptions and comparisons with independent observations made by other researchers.

The model predicts that vertical polarization will give higher normalized radar cross sectional values while higher frequencies will give higher values only for incidence angles (from the vertical) less than about 50°. It has yet to be determined whether other factors, (increased sea state return, increased atmospheric attenuation, etc.) will negate the benefit of using vertical polarization and higher frequencies in marine radars.

It has been shown that the average iceberg can be described as a very complex target, as such, it would be extremely difficult to apply the model accurately to individual icebergs to determine an estimate of the radar cross section. Because of the wide variation between individual icebergs this would be rather futile if the goal was to determine estimates of the cross sections of icebergs in general. The model can however be applied to iceberg models. Having characterized the surface on the microscale and provided a model it is necessary only to characterise the overall iceberg shape on the macroscale

and utilize standard modelling techniques to derive the total radar cross sectional value. For example, Barrick (1970) describes a method for determining the radar cross section for a slightly rough spherical surface. This same technique could be applied to obtain an estimate of the radar cross section for an iceberg presenting a spherical like surface to a radar. To obtain a radar cross sectional value for an iceberg presenting a vertical face (for example, a model of a tabular or blocky iceberg) to a radar the area of the surface could combined with the appropriate σ° value from Figure 18. The σ° value to be used would depend on, in this case, the horizontal orientation of the iceberg face with respect to the radar. Values of σ for complex shape models can be obtained using the methodology described by Crispin and Siegel (1968) and given in Section 5.4.

In summation, a model has been derived for the normalized radar cross section of a slightly rough glacial surface. The model can be applied on a practical basis to estimate radar cross sectional values for iceberg models. This information can be employed to provide a realistic estimate of the iceberg detection performance of individual marine radar configurations.

REFERENCES

Axline, R.M. Jr., and Mater, R. Theoretical And Experimental Study of Wave Scattering From Composite Rough Surfaces - First Annual Report, Task 1. A Contract Report Prepared for U.S. Army Topographic Laboratories. University of Kansas Space Technology Centre technical report no. 234-TR-234-2, 1974.

Barrick, Donald E. "Rough Surfaces," Vol. II of Radar Cross Section Handbook, edited by George T. Ruck. New York: Plenum Press, 1970.

Barrick, D.E. and Peake, W.H. Scattering from Surfaces with Different Roughness Scales; Analysis and Interpretation, Battelle Memorial Institute Research Report, November 1, 1967.

Benedict, C. Peter, and Hall, J.C.E. A Study of Iceberg Detection for Marine Navigation. A Contract Report Prepared for Transport Canada. Report No. TP2409, 1979.

Blake, Lamont V., Radar Range-Performance Analysis. Lexington: D.C. Health and Company, 1980.

Blenkarn, K.A., and Knapp, A.E. "Ice Conditions on the Grand Banks," The Ice Seminar. Published by the Canadian Institute of Mining and Metallurgy, Special Vol. 10, 1969.

Budinger, T.F. Ice Detection By Radar - Consolidated and Abridged Report. A Report Prepared by the International Ice Patrol. Woods Hole, Massachusetts: United States Coast Guard, 1959.

Budinger, T.F. "Iceberg Detection By Radar," International Ice Observation and Ice Patrol Service In the North Atlantic Ocean - Season of 1959, Bulletin no. 45. Washington: United States Government Printing Office, 1960.

Crispin, J. W., Jr, and Seigel, K.M. (editors). Methods of Radar Cross-Section Analysis. New York: Academic Press, 1968.

Cross, F.P., and Lewis J.R. CRC Radar Experiments Norploy '73: Phase I (Unclassified), Ottawa: Communications Research Centre (CRC Technical Note 664), 1973.

Dinsmore, Robertson P. Ice and its Drift into the North Atlantic Ocean. A Report Prepared for the International Commission for the Northwest Atlantic Fisheries, ICNAF Special Publication No. 8. Dartmouth, Nova Scotia, 1972.

Duval, Bernard C. "Exploratory Drilling on the Canadian Continental Shelf, Labrador Sea," Proceedings of the Seventh Annual Offshore Technology Conference, Houston, May 5-8, 1975. Houston, 1975.

Evans, S. "Dielectric Properties of Ice and Snow - A Review," Journal of Glaciology, Vol. 5, 1965.

Gray, A.L.; Hawkins R.K.; Livingstone, C.E.; Lowry, R.; Larson, R.; and Rawson, R. "The Influence of Incidence Angle on Microwave Radar Returns of 'Targets' in an Ocean Background," Proceedings of the Thirteenth International Symposium on Remote Sensing of Environment, Ann Arbor, Michigan, April 23-27, 1979, pp. 1815-1837.

Gray, A.L.,; Hawkins, C.E.; Livingstone, C.E.; and Arsenault, L.D. "Remote Sensing of Icebergs," Proceedings of the Second Workshop on the Microwave Remote Sensing of Sea Ice and Icebergs. Langley Research Center, Hampton, Virginia, 1981.

Gray, A.L. "Ice Hazard Detection, Modelling and Satellite SAR Image Simulation," Microwave Remote Sensing Meeting, Calgary, 30 November to 1 December, 1982. Prepared by the Canada Centre for Remote Sensing, Ottawa, January, 1983(a).

Gray, A.L., Personal Communication, November 1, 1983(b).

Hammond, R.E., II. Letter to B. Dawe, August 11, 1982.

Hood, A.D. An Analysis of Radar Ice Reports Submitted By Hudson Bay Shipping (1953). Ottawa: National Research Council of Canada, Electrical Engineering Division (ERB-330), 1953.

Hood, A.D. An Analysis of Radar Ice Reports Submitted By Hudson Bay Shipping (1954). Ottawa: National Research Council of Canada, Electrical Engineering Division (ERB-356, NRC No. 3560), 1954.

Hood, A.D. An Analysis of Radar Ice Reports Submitted By Hudson Bay Shipping (1955). Ottawa: National Research Council of Canada, Electrical Engineering Division (ERB-394), 1955.

Hood, A.D. An Analysis of Radar Ice Reports Submitted By Hudson Bay Shipping (1956). Ottawa: National Research Council of Canada, Electrical Engineering Division (ERB-416, NRC No. 4263), 1956.

Hood, A.D. An Analysis of Radar Ice Reports Submitted By Hudson Bay Shipping (1953-1957). Ottawa: National Research Council of Canada, Radio and Electrical Engineering Division (ERB-467, NRC No. 4692), 1958.

Jonasson, W.B.; Durand, C.; and Audette, M. "An Ice Hazard Detection System - Preliminary Investigation," Proceedings of the Sixth International Conference on Port and Ocean Engineering Under Arctic Conditions, Quebec City, 1981. pp. 1227-1238.

Le Page, L.S. and Milwright, A.L.P. "Radar and Ice", The Journal of the Institute of Navigation, Vol. 6, No. 2 (April, 1953) pp. 113-130.

Lewis, John C. and Benedict, C. Peter, "Iceberg Detection for Canadian Frontier Production," Proceedings of the Thirteenth Annual Offshore Technology Conference, Houston, 1981, pp. 115-121.

Long, Maurice W. Radar Reflectivity of Land and Sea. Lexington: D.C. Heath and Company, 1975.

Miller, J., "Ice Hazard Detection - Petro-Canada." Ice Remote Sensing Information Meeting, St. John's, 3 November, 1981. Prepared by the Canada Centre for Remote Sensing. Ottawa, January, 1982.

Murray, John E. "The Drift, Deterioration and Distribution of Icebergs in the North Atlantic Ocean," The Ice Seminar. Published by the Canadian Institute of Mining and Metallurgy, Special Vol. 10, 1969.

Nathanson, Fred E. Radar Design Principles. New York: McGraw-Hill Inc., 1969.

Peak, W.H. Theory of Radar Return from Terrain," 1959 IRE Convention Record, Vol. 7, 1959, pp. 27-41.

Pearson, D.; Livingstone, C.E.; Hawkins, R.K.; Gray, A.L.; Arsenault, L.D.; Wilkinson, T.L.; and Okamoto, K. "Radar Detection of Sea-Ice Ridges and Icebergs in Frozen Oceans at Incidence Angles From 0° to 90°," Proceedings of the Sixth Canadian Symposium on Remote Sensing, Halifax, 1980, pp. 231-241.

Pearson, D.E., "Role of Marine Radar within Petro-Canada's Ice Management Programme." Microwave Remote Sensing Meeting, Calgary, 30 November to 1 December 1982. Prepared by the Canada Centre for Remote Sensing, Ottawa, January, 1983.

Perry, R.E. "A Record of Radar Performance in Ice Conditions," The Journal of the Institute of Navigation, Vol. 6, No. 2 (April, 1953) pp. 74-85.

Remotec Applications Incorporated. An Assessment of Impulse Radar as an Iceberg Draft Measurement Tool. A Contract Report Prepared for the Centre for Cold Ocean Resources Engineering (C-CORE). C-CORE pub. no. 82-8. November, 1982.

Rice, S.O. "Reflection of Electromagnetic Waves by Slightly Rough Surfaces," Communications on Pure and Applied Math, Vol. 4, 1951, pp. 351-378.

Rice, S.O. "The Reflection of Electromagnetic Waves from a Rough Surface," The Theory of Electromagnetic Waves, edited by M. Kline. New York: John Wiley (Interscience), 1951; also New York: Dover, 1963.

Skolnik, Merrill I. (ed.) Radar Handbook. New York: McGraw-Hill Book Company, Inc., 1970.

Skolnik, Merrill I. Introduction to Radar Systems. 2nd ed. New York: McGraw - Hill Book Company, 1980.

Williams, P.D.L. "Detection of Sea Ice Growlers by Radar," Proceedings of the International Conference on Radar--Present and Future, London, England October 23-25, 1973. London: Institute of Electrical Engineers, 1973.

Williams, P.D.L. "The Detection of Ice at Sea by Radar," The Radio and Electronic Engineer, Vol. 49, No. 4 (June, 1979) pp. 275 - 287.

Wylie, F.J. The Use of Radar at Sea, revised edition. London: Hollis and Carter, 1968.

APPENDIX

CALCULATIONS REGARDING EMPIRICAL FITTING OF MODEL TO 13.3 GHZ DATA AND EXTRAPOLATION TO 9.5 GHZ

A.1. EMPIRICAL FITTING OF THE MODEL TO 13.3 GHz DATA

The applicable average incoherent normalized radar cross sectional model equations are:

$$\sigma_V = \left| \frac{4.84 \sin^2\theta + 7.04}{\left[3.2 \cos\theta + \sqrt{3.2 - \sin^2\theta}\right]^2} \right|^2 \cdot X \qquad (A1)$$

$$4 k^4 h^2 \ell^2 \cos^4(\theta) \exp(-k^2 \ell^2 \sin^2\theta)$$

$$\sigma_H = \left| \frac{2.2}{\left[\cos\theta + \sqrt{3.2 - \sin^2\theta}\right]^2} \right|^2 X \qquad (A2)$$

$$4 k^4 h^2 \ell^2 \cos^4(\theta) \exp(-k^2 \ell^2 \sin^2\theta)$$

where v, H denote vertical and horizontal polarization, respectively,

$k = 2\pi/\lambda$, the free space wave number,

λ is the radar frequency wavelength,

h is the root mean square surface height roughness,

ℓ is the correlation length, and,

θ is the angle of incidence with respect to the vertical.

It has been stated that although the model did not fit measured data well in absolute terms it did accurately predict the variations with incidence angle, frequency and

polarization on a relative basis. Therefore, the initial objective here is to determine the model parameters which result in the curve that best fits the measured data.

Examination of equations (A1) and (A2) shows that h and ℓ are the only two unknown factors. The parameter, h, however, only effects the overall amplitude and does not effect the shape of the curve. Therefore it can be set to a value of 1.0. The parameter, ℓ, effects both amplitude and shape. However, in actuality a value for the factor, $k\ell$, needs only to be determined.

Column (2) of Table A1 provides the measured values obtained for the various incidence angles (column (1)) at 13.3 GHz (2.25 centimetre wavelength) using vertical polarization. After initial trial and error calculations using equation A1 it was found that $k\ell$ values ranging from 2.0 to 2.2 provided curves that closely matched the shape of the measured data variation with incidence angle (Figure A1). Using the 8.0° measured value (-5.0 db) as a pivot point (that is, the model value at the corresponding angle was set equal to this value and all other values were determined and adjusted relative to this point), the values shown in columns (3), (5), and (7) were determined for $k\ell$ values of 2.0, 2.1 and 2.2, respectively.

To determine which curve was the best fit the sum of the absolute values of the differences between the actual

TABLE A1 - COMPARISON OF MODEL VALUES WITH MEASURED DATA (13.3 GHZ VERTICAL POLARIZATION) FOR $k\ell$ = 2.0, 2.1, AND 2.2 USING THE 8.0° MEASURED VALUE AS A PIVOT POINT

(1) Angle of Incidence (degrees)	(2) Measured σ° Value (db)	(3) Model Value For $k\ell$ = 2.0 (db)	(4) Difference (3) - (2) (db)	(5) Model Value For $k\ell$ = 2.1 (db)	(6) Difference (5) - (2) (db)	(7) Model Value For $k\ell$ = 2.2 (db)	(8) Difference (7) - (2) (db)
8.0	-5.0	-5.0	-----	-5.0	-----	-5.0	-----
14.4	-5.0	-5.6	-0.6	-5.7	-0.7	-5.7	0.7
24.9	-7.5	-7.3	+0.2	-7.5	0	-7.8	0.3
34.9	-11.0	-9.6	+1.4	-10.1	+0.9	-10.7	-0.3
44.9	-14.0	-12.5	+1.5	-13.4	+0.6	-14.3	0.3
55.5	-16.3	-16.4	-0.1	-17.6	-1.3	-18.8	2.5
Sum of Absolute Value of Differences			3.8		3.5		4.1

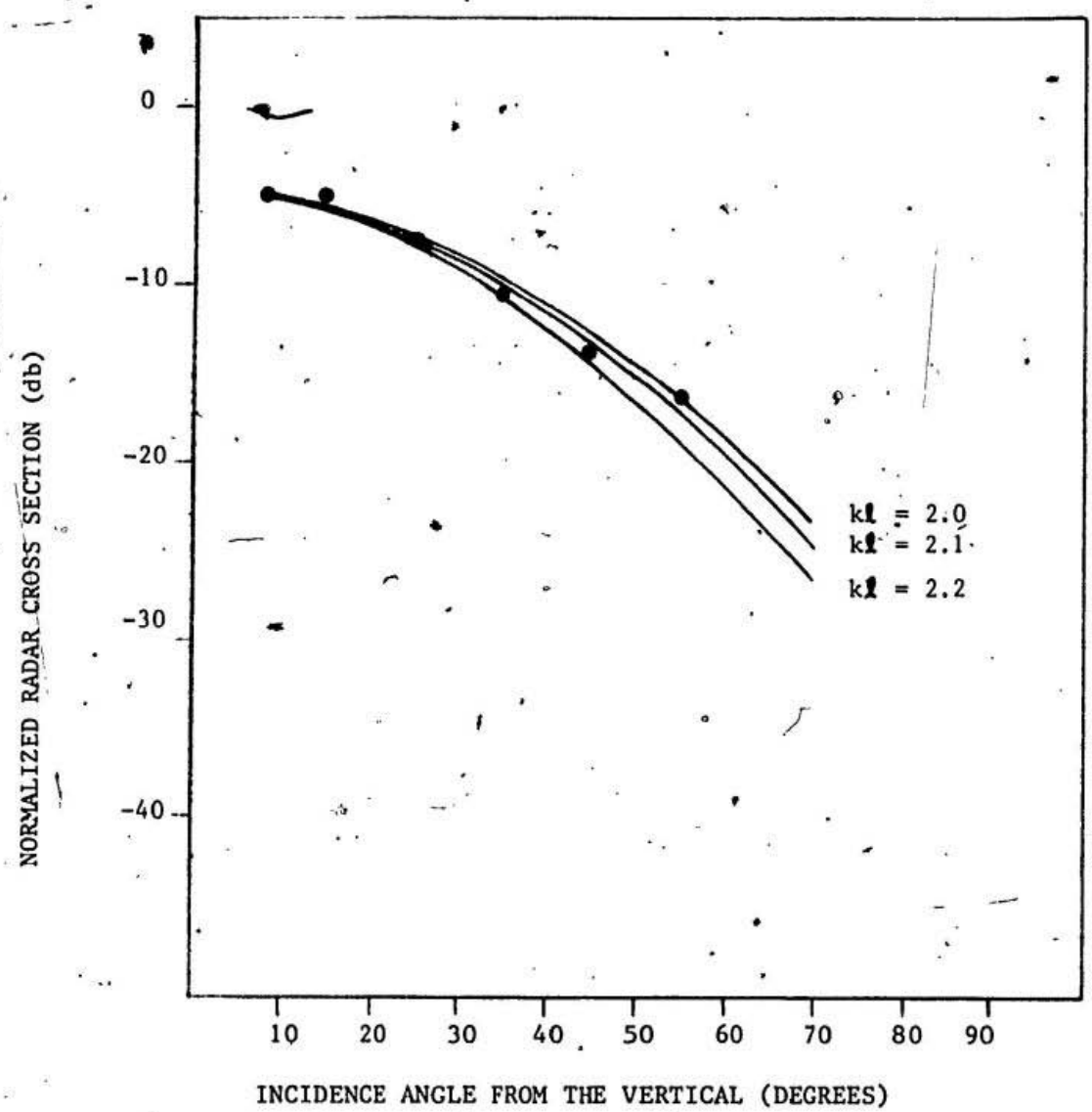

FIGURE A1 - COMPARISON OF FIT TO ICEBERG DATA USING THREE kℓ VALUES WITH SLIGHTLY ROUGH SURFACE MODEL

model value at each angle were obtained (residuals) for each $k\ell$ value and are shown in the bottom of Table A1. The $k\ell$ value of 2.1 gave the smallest value and is therefore said to fit the shape of the data variation best.

Having selected the curve using $k\ell = 2.1$ as the best shape fit it is necessary to fit the curve absolutely to the data. This was accomplished first by obtaining the sum of the excursions in column (6). A net excursion of 0.5 db was obtained. The best fit is assumed to have a net excursion value of 0 db. By shifting each value by 0.1 db it was found that this was achieved. The model values for the best fit curve ($k\ell = 2.1$) are shown in Table A2.

To determine the goodness of the fit a Chi-square test was performed. Table A3 shows the results of the calculations to determine the chi-square value of 0.28. Using 5 degrees of freedom and a 5% level of significance, the actual chi-square value for 95% confidence level is 11.07 (from statistical tables). Therefore the curve is shown to be a very good fit to the data.

A.2 DETERMINATION OF VALUES FOR HORIZONTAL POLARIZATION

Equations (A1) and (A2) are equal at 0° incidence. Therefore in order to determine values for horizontal polarization it is only necessary to utilize equation (A2) and adjust the values obtained for each angle relative to

TABLE A2 - NORMALIZED RADAR CROSS SECTION VALUES DERIVED FOR 13.3 GHz USING VERTICAL POLARIZATION AND OBTAINED BY EMPIRICALLY FITTING MODEL TO CURVE DESCRIBED BY MEASURED DATA

Incidence Angle (Degrees)	σ_v° (Decibels)
0.0	-4.6
8.0	-4.9
10.0	-5.1
14.4	-5.6
20.0	-6.4
24.9	-7.4
30.0	-8.7
34.9	-10.0
40.0	-11.7
44.9	-13.3
50.0	-15.3
55.5	-17.5
60.0	-19.5
70.0	-24.8
80.0	-33.7

TABLE A3 - CALCULATION OF CHI-SQUARE VALUE FOR GOODNESS OF FIT TEST

x Measured Value (db)	y Model Value (db)	$(x-y)^2/y$
-5.0	-4.9	0.002
-5.0	-5.6	0.064
-7.5	-7.4	0.001
-11.0	-10.0	0.100
-14.0	-13.4	0.027
-16.3	-17.5	0.082
CHI-SQUARE VALUE		0.276

the value of -4.6 db obtained for 0° and shown in Table A2. The results are tabulated in Table A4.

A.3 - EXTRAPOLATION DOWN TO 9.5 GHz

In Section A.1 a value of $k\ell = 2.1$ was found to provide a reasonable fit of the model to the measured data. The wave number, k, is known and equal to 2.793/centimetre. Therefore, the value of ℓ can be derived and is found to be equal to 0.752 centimetres. This value is independent of frequency. It is now possible to derive a $k\ell$ value at 9.5 GHz (3.2 centimetres). The wave number at this frequency is 1.963/centimetre, resulting in a $k\ell$ value of 1.48.

The only difference in Equation (A1) and (A2) resulting from a change in frequency at 0° incidence is the change caused by the k^4 term which is 60.81 for 13.3 GHz and 14.86 for 9.5 GHz. The effective change in decibels is 10 log (14.86/60.81) = -6.13 db. Therefore the 9.5 GHz value at 0° incidence is just 6.13 db lower than that of 13.3 GHz or -10.7 db (using the 0° value in Table A2). Using this value the same technique as was employed in Section A-2 can be applied with equation (A1) to determine values for 9.5 GHz (vertical polarization). These are tabulated in Table A5. Horizontal polarization values can be determined using the same technique as

TABLE A4 - NORMALIZED RADAR CROSS SECTIONAL VALUES AT 13.3 GHz (HORIZONTAL POLARIZATION) DERIVED FROM THE MODEL

Angle of Incidence (Degrees)	σ° (Decibels)
0	-4.6
10	-5.3
20	-7.3
30	-10.6
40	-14.8
45	-17.2
50	-19.9
60	-25.8
70	-33.2
80	-44.6

TABLE A5 - NORMALIZED RADAR CROSS SECTIONAL VALUES DERIVED FOR 9.5 GHz (VERTICAL POLARIZATION) BY EXTRAPOLATION DOWN FROM 13.3 GHz USING THE MODEL

Angle of Incidence (Degrees)	σ_v° (Decibels)
0	-10.7
10	-10.9
20	-11.4
30	-12.4
40	-13.8
45	-14.7
50	-15.7
60	-18.4
70	-22.4
80	-30.4

employed in Section A.2 for that polarization and Table A6 provides these results.

TABLE A6 - NORMALIZED RADAR CROSS SECTIONAL VALUES AT 9.5 GHz (HORIZONTAL POLARIZATION) DERIVED FROM THE MODEL

Angle of Incidence (Degrees)	σ_H° (Decibels)
0	-10.7
10	-11.1
20	-12.4
30	-14.2
40	-16.9
45	-18.5
50	-20.3
60	-24.7
70	-30.7
80	-41.4